Dissertation Title:

TECHNICAL FEASIBILITY STUDY OF THE USE OF A STATCOM AND SSSC TO OPTIMIZE THE STABILITY OF RWANDAN ELECTRICAL GRID

CASE STUDY: KIGALI HIGH VOLTAGE NETWORK

By

ICYUZUZO Alain Colombe

Student Registration number: 221030395

A dissertation submitted in partial fulfillment of the requirements for the Degree of

MASTER OF SCIENCE IN ELECTRICAL POWER SYSTEMS

In the African Center of Excellence in Energy for Sustainable Development,

College of Science and Technology

Supervisor:

Dr. Jean Marie Vianney BIKORIMANA

December 2023

DECLARATION

I declare that this Dissertation contains my own work except where specifically acknowledged, and it has been passed through the anti-plagiarism system and found to be compliant and this is the approved final version of the Dissertation.

Student name: ICYUZUZO Alain Colombe

Registration number: 221030395

Signed……………………………………………………….

Date: 4th December 2023

Main Supervisor Name: Dr. Jean Marie Vianney BIKORIMANA

Signed……………………………………………………….

Date: ……………………8th December 2023……………………...

ABSTRACT

The electricity plays a great role in the human activities and in every community. The wide-ranging applications of modern, affordable, reliable, and sustainable electrical energy services can contribute to the poverty eradication and socio-economic development in Rwanda.

The Rwandan electrical grid is similar to the most of worldwide countries. It is composed of generation power plants, substations and load that are interconnected by transmission and distribution lines at different voltage levels. The Government of the Republic of Rwanda has initiated different national targets in order to expand the grid with 556MW generation capacity and 100% electricity access by 2024 [1]. The grid will thus become larger and robust to satisfy the highly increasing number of future electricity consumers.

Unfortunately, there is a risk that the electric grid will face instability problems along with the amplified power losses from outages and power services delivery to electricity users, especially in high load centers, including Kigali City and industrial areas. It is crucial to plan and execute the future electric infrastructures which can operate at their capacity limits to satisfy both load and socio-environmental requirements. This performance can be achieved by the use of FACTS based technology to improve the network stability and power transfer capabilities.

This study finds out an efficient way to build a resilient electrical grid which has the capability to control the voltages and damp the transients on high voltage buses in Kigali region after the occurrence of an electric disturbance by using FACTS controllers “Static Synchronous Compensator (STATCOM)” and “Static Synchronous Series compensator (SSSC)”.

In order to reach the expected network performance, the Rwandan high voltage network and past network disturbances have been assessed and the electrical quantities which will be required to control the future network stability have been identified with FACTS Controllers. Furthermore, the future network with FACTS controllers is simulated by using Simulink in order to check the systems behavior by creating disturbances on the different power supplies. At the end, the results have been interpreted and compared to display the stability improvement.

Keywords: Rwandan grid, system stability, power flow, FACTS, Simulation

LIST OF SYMBOLS AND ACRONYMS

ABBREVIATIONS

Terms	**Nomenclature**
AC	Alternating Current
ACEESD	African Center of Excellence in Energy for Sustainable Development
CoD	Commercial Operation Date
CSC	Current Source Converter
DC	Direct Current
DPFC	Dynamic Power Flow Controller
DVR	Distributed Voltage Regulator
EUCL	Energy Utility Corporation Limited
ESSP	Energy Sector Strategic Plan
FACTS	Flexible Alternating Current Transmission System
FC	Fixed Capacitor
FY	Financial year
GTO	Gate Turn-Off
GUPFC	Generalized Unified Power Flow Controller
HPFC	Hybrid Power Flow Controller
HV	High Voltage
HFC	Hybrid Flow Controller
IGBT	Insulated-Gate Bipolar Transistor
IPFC	Interline Power Flow Controller
LV	Low Voltage
MSC	Mechanically Switched Shunt Capacitors
MV	Medium Voltage
NISR	National Institute of Statistics of Rwanda
Nos	Number
NST1	National Strategy for Transformation 2017-2024
PI	Proportional-Integral
PLL	Phase-Locked Loop
PWM	Pulse Width Modulation

PSS®E	Power System Simulator for Engineering
PST	Phase Shifting Transformer
PQ	Power Quality
RBF	Radial Basis Function
REG	Rwanda Energy Group
RWF	Rwandan Francs
SCADA	System Control and Data Acquisition
SMIB	Single-machine Infinite-Bus
SPLK	Shema Power Lake Kivu
SSSC	Static Synchronous Series Compensator
SVC	Static Var Compensator
STATCOM	Static Synchronous Compensator
S/S	Substation
TL	Transmission Line
TCR	Thyristor Controlled Reactor
TCSC	Thyristor Controlled Series Compensator
TCPST	Thyristor Controlled Phase Shifting Transformer
TPSC	Thyristor Protected Series Compensator
TSC	Thyristor-Switched Capacitor
TSSC	Thyristor-Switched Series Capacitor
TSSR	Thyristor Sub-Synchronous Resonance
UETCL	Uganda Electricity Transmission Company Limited
UPFC	Unified Power Flow Controller
UoM	Unit of Measure
UR	University of Rwanda
VAR	Volt-Ampere reactive
VSC	Voltage Source Converter
W	Watt
WSCC	Popular Western System Coordinated Council

SYMBOLS

Symbol	Meaning
P	Active Power
Q	Reactive Power
S	Apparent Power
B	Susceptance
R	Resistance
X	Reactance
Z	Impedance
A	Ampere
I	Current
V	Voltage
Ω	Ohm
B_m	Flux loss
G_m	Eddy Current Loss
&	And
p.u	Per Unit
%	Percentage
Prefix: T, G, M, k, m, μ	Tera, Giga, Mega, Kilo, Mili, Micro

TABLE OF CONTENTS

LIST OF TABLES

LIST OF FIGURES

CHAPTER 1. GENERAL INTRODUCTION

1.1.BACKGROUND

The need of electrical energy is highly increasing because this clean energy has different applications in all activity sectors in Rwanda and it is contributing to the economic development and social transformation.

The electrical energy can be generated by different power sources and transmitted to the end users through interconnected electrical components including but not limited to substations, transmission, and distribution lines. Such interconnected infrastructures form one electrical grid with different voltage levels and hence, it requires an efficient way to control the stability of the entire system in order to avoid any power interruption.

The integration and development of FACTS technology in Rwandan network can be the best option to improve the power system capability, meet socio-environmental requirements and lastly, reduce the costs which will be associated for outages.

1.2.PROBLEM STATEMENT

The network instability is mainly caused by small perturbations which may be caused by load variation and high perturbations from faults and loss of synchronization of big generators, connected in the network [2].

In this regard, EUCL has indicated that the power system is still encountering emergency and mal-operation situations whereby the transmission line tripping or overloading, voltage collapse, quick-frequency declines, lightning strikes are among the main causes of power system blackouts [3]. So far, REG has reported the remarkable financial losses from the network disturbances whereby they have been increased from 444,517,432 Rwf during FY 2019-2020, 441,882,913 Rwf during FY 2020-2021, and 473,094,993 Rwf during FY 2021-2022 [1]. Therefore, by using the Lagrange's extrapolation method, the expected financial losses are expected to be 2,646,778,760 Rwf by 2032 in no action is taken at the moment.

On the similar note, there are high relative energy costs and unreliable power supply which disincentivize stronger industrial growth and business expansion [4]. The main causes are identified without limitation as the inadequate infrastructures which require a huge investment, sound demand-supply imbalance and fuel-based electricity generation.

One of immediate solutions under implementation is to increase the capacity of generation, transmission, and distribution infrastructures to satisfy the existing and future load. Unfortunately, it becomes more difficult at a certain level to expand the grid due to environmental and social constraints.

Other raised challenges are:

- High power losses which are at 18.10% as per June 2022 from 19.26% by June 2021, in addition to 4 blackouts which have been experienced in FY 2021-2022 [1].
- The power generation resources are limited especially during dry season when many hydropower plants face water shortage problems whereas rental diesel generation is used to supply the peak demand which comes at a high cost [4].
- High rate of population growth in Rwanda, whereby 60.98% increase is expected for 20 years period (from 2012 to 2032) and after this period, the population size will not vary tremendously according to NISR report [5]. Therefore, the annual growth can be estimated more than 3.049% and the associated living requirements, including the need of electricity, can be assumed at the same rate as well.

The existing scenario shows that the Rwandan network has many stability problems which rise up due to the remarkable network expansion to fulfil the future electricity demand. Consequently, there will be a great probability of network collapse, additional operation costs and financial losses from the increase in electrical disturbances.

Therefore, the alternative solution which will become mandatory is to plan and execute new electric infrastructures which can operate at their limits to fulfill both load and socio-environmental requirements. And FACTS based technology under this study gives another reflection to reduce the effects from the above-mentioned risks.

1.3.OBJECTIVE

1.3.1. GENERAL OBJECTIVE

The general objective is to improve the stability of Rwandan grid by using the combination of SSSC and STATCOM as hybrid power flow controller to regulate power flow through controlling voltages and damping the transients in Kigali HV network.

1.3.2. SPECIFIC OBJECTIVES

The specific objectives of this research are:

- To investigate the level of stability of the existing Kigali HV network
- To predict the financial losses which are linked with the existing Kigali HV network.
- To model the existing Kigali HV network with integration of a STATCOM and SSSC
- To simulate the existing Kigali HV network with and without the integration of a STATCOM and SSSC

1.3.SCOPE OF STUDY

This research focuses on the analysis and simulation of electrical parameters which are collected from different transmission lines and substations in Kigali HV network. Then, the obtained results of conventional HV system are compared with the future network which is developed and simulated with FACTS Controllers to display the improvement.

1.4.INTENDED OUTCOME AND SIGNIFICANCE OF STUDY

1.4.1. EXPECTED AOUTCOME

This study offers the actual and future abnormal characteristics of the existing conventional HV network against different electrical disturbances. As result, the study elaborates the power electronics-based model which uses the integrated hybrid power flow controller and associated key considerations for the future power stability improvement in Kigali HV network.

1.4.2. SIGNIFICANCE OF THE STUDY

Since this research assesses the real time and forecasted data and elaborate the simulated comparative model; the findings from this study will reflect and help REG for the improvement of HV master plan, to effectively solve the network instability challenges ahead of time while providing good services to their clients, including both big and small consumers of electrical energy. Besides, the analysis from this study provides the relevant details to Government of

Rwanda, investors, consultants, contractors, researchers for further development of the national grid to solve future power quality issues.

1.5.DISSERTATION OUTLINES

The present dissertation has five chapters:

Chapter 1: “General introduction” which provides a good understanding of the activities of the research project that are relative to the topic and covers the impression of the whole work.

Chapter 2: “Literature review on high voltage power network” offers the description of the architecture, characteristics, and applications of the existing power flow controllers to stabilize the network. In addition, the existing network components, traditional way for voltage control as well as actual and future change of electrical parameters of the electrical high voltage network in Kigali City are identified and assessed.

Chapter 3: “Methodology” describes the procedures, data and tools which have been used to reach the obtained results.

Chapter 4: “Modelling and Simulation of Kigali high voltage network with STATCOM and SSSC controller” provides a mathematical and simulated model of Kigali High Voltage network with “STATCOM” and “SSSC” to optimize network voltage stability.

Chapter 5: “Conclusion and recommendations”, as the last chapter of the study, summarizes the achieved goals on the stability improvement and provides some key considerations and recommendations for the next similar projects.

CHAPTER 2. LITERATURE REVIEW ON HIGH VOLTAGE POWER NETWORK

2.1.INTRODUCTION

In order to balance the generation and demand, the electrical network will require enough electrical lines to transport the electricity as well as substations to facilitate the electrical operation since the electricity cannot be stored in important amount. Unfortunately, the continuous expansion of electric network and their associated interconnections with the use of the traditional development, may cause complexities in operation and consequently, the operation methods become limited.

In fact, the optimal active and reactive power flow can be achieved by controlling the transmission line parameters such as impedance, the magnitude of the terminal voltages, and the phase angle between the voltages.

This chapter provides some reviews to identify suitable FACTS devices which can improve Kigali HV network to operate closer to its stability limits in order to prevent power instability problems.

2.2.OVERVIEW OF POWER FLOW CONTROLLERS

Many researchers have worked on power flow controllers to overcome the power system instability problems from ever-growing electricity demand with population and modernization growth. In many countries, the authorization to construct new transmission lines are hard to get, and thus the existing network has to be enforced to fulfill the changing requirements [6] which can be achieved by the use of FACTS controllers.

FACTS controllers have various applications, but this study will be limited to network voltage control by the means of shunt and series compensation of reactive power.

2.2.1. RELATED WORKS ON FACTS CONTROLLERS

B. Valani (2016), presented the enhancement of voltage stability using STATCOM and SSSC. The research was mainly intended to investigate the effect of STATCOM and SSSC in controlling active and reactive powers to maintain voltage stability at various buses by using PI Controller in MATLAB/Simulink environment. The SSSC is connected in series with the transmission line and composed of a coupling transformer, voltage source converter and DC capacitor. The operation of the SSSC was achieved by varying the effective impedance of a line through the injection of a voltage containing an appropriate phase angle in relation to the line current. The exchange real power is achieved if the injected voltage is in phase with the line current and on the other hand, the exchange of reactive power is achieved if a voltage is injected in quadrature with the line current. The study displayed that the SSSC is a more potential and beneficial controller than other series controllers like TCSC because it has the capability to modulate both the line impedance in accordance with the power oscillations. The STATCOM is a shunt-connected device for reactive power compensation and comprises a coupling transformer, voltage source converter and DC capacitor like SSSC. The desired level of reactive power consumption and generation is achieved by controlling the current and voltage from a voltage source converter. The researcher thus simulated a two-machine power system model without FACT device, with SSSC and with STATCOM and the results proved that the active and reactive power as well as the voltage at each bus have been improved in the system and consequently, it found that the construction of the new transmission line would be no longer needed to satisfy the load requirements in case the SSSC and STATCOM are connected to the system [7]. Unfortunately, the test model is limited to two machines and four bus systems only in MATLAB/Simulink.

Pradeep H. Kathar (2019) studied the detailed description of the STATCOM and SSSC to reduce the electrical losses and improve the voltage profile in power system. The MATLAB/Simulink was used as a simulation tool to investigate and compare various electrical parameters, their control measurements. Afterwards, the general observation specified that the transfer capability of a transmission line can be improved if both shunt as well as series compensations are used. In similar note, SSSC was described as the most preferred dynamic controller to improve the voltage stability, but the selection of effective control strategy of SSSC is a key factor to reach the optimal stability. The simulation results showed that STATCOM provided higher power losses of 0.04564p.u which is reduced with SSSC up to 0.04362 p.u. Besides, the voltage stability has been tested by creating a three-phase fault by using fault creator and the voltage variation has thus been displayed and rectified by using STATCOM and SSSC. The results showed that the fault was cleared, and system became stable when SSSC and STATCOM were integrated [8]. Unfortunately, the components of the studied system are limited to one source, one transformer, two buses, one transmission line, one RLC load, a STATCOM and SSSC. This approach cannot assure that the real contribution of STATCOM and SSSC once they are applied in a system which contains multiple components of the same type.

Ghorbani A., et al. (2016) proposed a new method to protect the synchronous generator from Loss of Excitation (LOE) by the use of STATCOM and SSSC. In order to produce three-phase AC output voltage, the adequate DC voltage and current are required to excite the field windings of the generator. LOE can cause voltage collapse in the power system and occurs when a short or open circuit as well as some mistakes in control or operation of the system. Thus, the researchers used the STATCOM and SSSC so as to limit the decrease in output voltage by injecting the reactive power and therefore, cause a delay in the operation of LOE relay while preventing the damage of generator. All simulation results have been obtained in MATLAB/Simulink environment [9]. However, the researchers focused only on the application of both STATCOM and SSSC to ensure the voltage control and protection of a generator which is always at the sending end of the transmission system. The study failed to describe the proposed method in the complete system which comprises generation, transmission and load.

Antony et al. (2016) studied the use of Distributed Power Flow Controllers (DPFC), STATCOM and Dynamic Voltage Restorer (DVR) as FACTS devices to mitigate the voltage swell and sag of power quality issues due to the load and a wind turbine system. In fact, the power variation from renewable sources such as wind and solar can cause voltage fluctuations. Therefore, DPFC can play as a combined series-shunt compensator, which has a structure similar to UPFC, to prevent power quality problems. The MATLAB/Simulink results showed that test model of a combined DVR and STATCOM along with the conventional system provided shunt and series compensation by keeping 10-minute average of voltage fluctuation within $\pm 5\%$ of nominal value, and hence, the stability was controlled at the load side when a wind turbine is connected to the network. The STATCOM also used active filter to cancel the harmonics by injecting the exact current into the system at the point of common connection. The study discussed on Space Vector Pulse Width Modulation (SVPWM) as STATCOM control strategy to reach the effective voltage control [10]. However, the method was applied with wind generation system, which has other special design considerations.

Paul et al. (2016) proposed the use of PI-controlled SSSC to improve transient stability of the power system. The model of SSSC is composed of a series-connected transformer, the transmission line and a voltage source converter and a DC capacitor. Briefly, the research work concentrated on design of SSSC and its controllers where the circuit diagrams and dynamic equations were established to describe the system performance for series compensation of reactive power, and its relationship between the converter currents and voltages; the sending and receiving end voltage for transmission line [11]. The research has been found to be less contributive because the researchers focused mainly on a specific SSSC control scheme. In addition, only one controller and few numbers of network elements were discussed, whereas there are other controllers like STATCOM which can be simulated with SSSC to fulfill certain requirements of big network.

Ronita Pawn et al. (2016) assessed the capabilities of SSSC to control the flow of power at a particular point in the transmission line. The test models were composed of 4 and 6 IEEE bus systems in MATLAB/Simulink environment, whereby SSSC has been installed to inject a fast-changing active voltage in series with the line irrespective of the phase and magnitude of the line current to damp power oscillation on a grid power system. And the obtained results with and without SSSC have been compared graphically. Unfortunately, the study did not interpret the graphical results to showcase a clear improvement [12].

Adepoju et al. (2018) studied the application of SSSC to the 330kV Nigerian transmission network in order to control the voltage fluctuations the same as solving the network overloads, and losses problems. The simulation results showed that, the network active power loss was reduced by more than 5% whereas the voltage magnitudes have been improved to a specified value at buses the SSSC was effective in eliminating voltage limit violation, control bus voltage magnitude to specified value. An instance can be observed at bus 14, whereby the observed voltage magnitude was improved from 0.9462p.u. to 1.00p.u after incorporation of SSSC [13]. The shunt compensation is however missing in the performed research.

Yadav et al. (2017) proposed a Matlab/Simulink model for the improvement of the steadiness of the generators' rotor. In fact, the network becomes stable in three different ways. The first way is the generator's ability to remain in synchronism after a system disturbance whereby both input electromagnetic and output mechanical torques must be always in equilibrium to allow rotor angle stable. Secondly, the voltage must also be stable on all system's buses after disturbance or in steady state conditions. Lastly, the balance between power supply and demand. The researchers assessed the impact from the integration of FACTS controllers like SVC, TCSC and SSSC on the rotor, which resulted effective voltage stability on a system with 3 generators and 9 buses [14].

Gaurav K., Sunil R.W., Bapina D. Sh. (2016) proposed the use of STATCOM to compensate the relative power and prevent the power system harmonics in Matlab/Simulink environment. Proportional Integral and hysteresis control have been used as well as strategy to modify power system parameters and hence reach higher stability. In fact, an AC source, power line and unbalanced load have been simulated without and with STATCOM and then single-phase fault has been applied and the researchers compared the results. It was observed that the STATCOM injects current into the power system to compensate the sag and absorbs the current from the system when there is swell [15]. However, this research studies DSTATCOM as FACTS which can contribute to the improvement of the quality of power at distribution level.

Ronita P. and Thakre R. B. (2016) compared the stability results from the simulation of 4 and 6 IEEE Bus systems with SSSC in Matlab/Simulink environment. In fact, the use of SSSC can help to overcome the power system voltage collapse due to heavy loaded conditions. To achieve the appropriate results, the calculation of active and reactive power of the bus have been made by the use of PI controllers [12].

2.2.2. COMPARISON BETWEEN CONVENTIONAL AND FACTS DEVICES

This section focuses on the comparison of different FACTS devices and the conventional power flow controllers, in terms of definitions, types, construction, performance as well as the cost range.

The conventional devices are primarily fixed or mechanically switched reactors or capacitors which are connected in shunt or in series with a transmission line for the reactive power compensation. In this regard, the reactors are installed in order to minimize the overvoltage in a line in case of light load conditions whereas the capacitors are also used to stabilize the power line's voltage level during heavy load period. The AC power tends to be increased during its transport. Therefore, series-connected conventional devices can also be used to maintain the power flow at the required level over long distances. The PST is given as a well-known shunt-series device which is used to control power flows in transmission lines whereby it provides a supplementary phase shift between the sending and receiving end voltages. However, the conventional devices have slow control in nature and the switching frequency is limited as compared to FACTS devices [16].

Similarly, FACTS controllers are also used for series or shunt compensation of reactive power. But FACTS devices are power electronics-based controllers with a specific control design to fulfill the required operational conditions of the electrical network. They work electrically as fast current, voltage or impedance controllers because of the integrated power electronic which allows very short reaction times, and they have no moving parts.

The main application of the shunt devices is for reactive power compensation and therefore voltage control, whereas the series devices help to compensate the reactive power and influence the effective impedance on the line and consequently, on the stability and power flow. In similar note, shunt-series devices can simply help to control the power flow.

SVC is a widely used as shunt FACTS device and consists of a combination of fixed capacitor (FC) or thyristor-switched capacitor (TSC) in conjunction with thyristor-controlled reactor (TCR) to compensate the shunt reactive power. SVC is based on thyristor without the gate turn-off capability and cheaper, but SVC has lower performance and higher MVA size as compared to STATCOM.

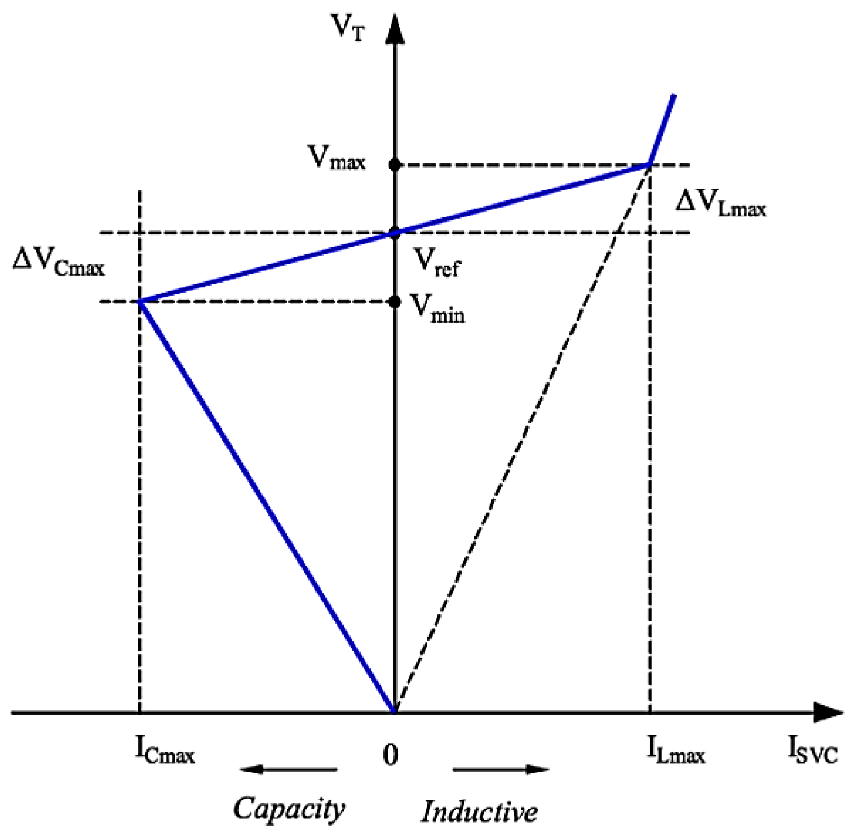

Figure 2.1: V-I characteristics of SVC [17].

The cost range of SVC is $20-$45/kVAR [18]. The characteristic of SVC is displayed in figure 1. In fact, the SVC is practically used to allow the terminal voltage (ΔV_{Cmax} or ΔV_{Lmax}) varies in proportion with the compensating current (I_{Cmax} or I_{Lmax}). In addition, V_T and I_{SVC} stand for line voltage and the injected SVC current respectively. And V_{ref} is the reference voltage at which the SVC can neither absorbs nor generates reactive power into the power system.

TCSC is composed of the combination of FC and TCR with mechanically switched capacitor banks in series in order to control the effective line reactance. As well, the cost range of TCSC is $25-$50/ kVAR [18].

STATCOMs are like SVCs except that they use GTO thyristors as electronic switches. In addition, STATCOM do not require large inductive and capacitive components to provide inductive or capacitive reactive power to high voltage transmission systems. Lastly, STATCOM has the higher reactive output at low system voltages whereby the STATCOM current is independent from the system voltage. The cost range is $80-$100/ kVAR [18]. The details for the STATCOM have been studied and described in section 2.2.3 of this research report.

SSSC is a voltage source inverter which is connected in series with a transmission line by the means of coupling transformer to inject a sinusoidal voltage, of variable magnitude in quadrature, with the line current to control the power flow. The detailed description of SSSC is included in the scope of this research and provided in section 2.2.4.

UPFC consists of a voltage source, inserted in series with the line and a current source, connected in shunt with the line. In fact, UPFC is simply a combination of STATCOM and SSSC, which are coupled via a common DC link, to allow bi-directional flow of real power between the series output terminals of the SSSC and the shunt output terminals of the STATCOM and are controlled to provide concurrent real and reactive series line compensation without an external electric energy source as shown in figure 1. The controllable parameters are magnitude and the angle of inserted voltage as well as magnitude of the current. By referring to the use of figure 1, $I_f, V_f, I_p, V_p, I_s, V_s, I_t, V_t$ V_{dc} and V_{dc} stand for sending-end current, sending-end voltage, STATCOM current, STATCOM voltage, line current, SSSC voltage, receiving-end current, receiving-end voltage and output voltage of DC system respectively.

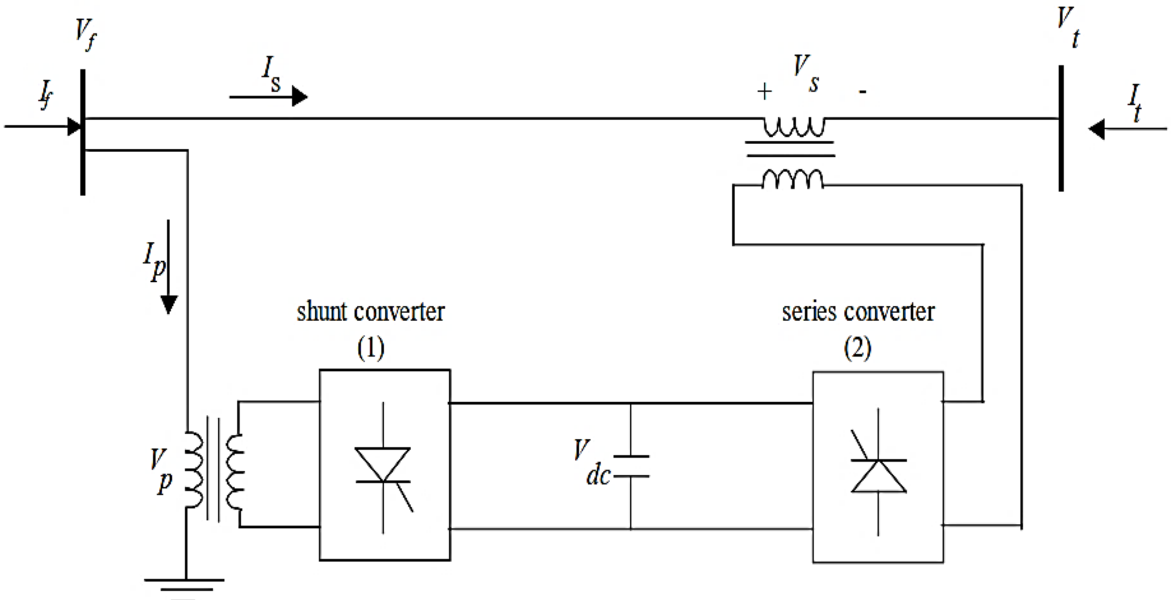

Figure 2.2: The equivalent circuit of UPFC

In fact, the entire system comprises two GTO converters (1 and 2), a common DC circuit as well as shunt and series transformers. The role of shunt converter is to provide the real power demand of series converter at the common DC line terminal from the AC side, whereas the series converter generate a voltage source at the fundamental frequency with variable amplitude and phase angle to the line by the means of boosting transformer and therefore, facilitate in series compensation of reactive power and the voltage control. The cost range of UPFC is \$150-\$200/kW [18].

Finally, most of the other FACTS devices combine two or more converter blocks like interline power flow controller (IPFC) and the generalized unified power flow controller (GUPFC) in order to ensure the required flexibility. The IPFC is simply a combination of two or more SSSCs which are connected through a common DC link in order to enable the real power flow between the AC terminals of the SSSC. This configuration helps to adjust the real power flow at each transmission line as well as balancing reactive power flow among the lines independently. The figure 2.3 shows two SSSCs which are connected in series between buses m_1 and m_2 and linked with a DC capacitor. V_{s1} and V_{s2} stand for series voltages of SSSC 1 and SSSC 2 respectively. The bus f may be installed between two controllers so that it can be monitored as well.

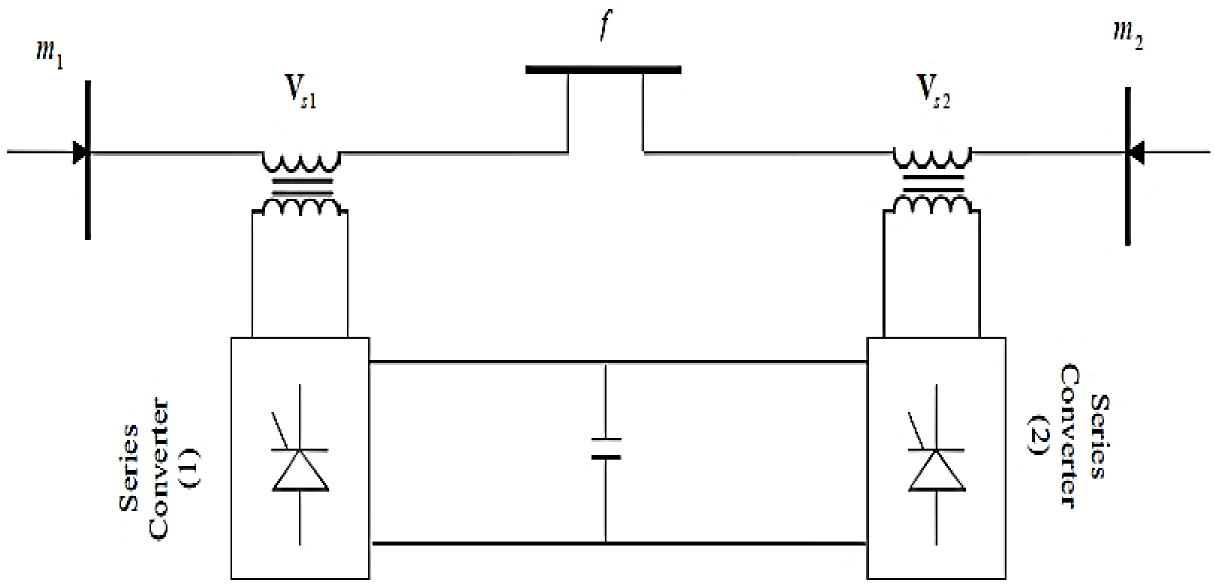

Figure 2.3: Equivalent circuit of IPFC

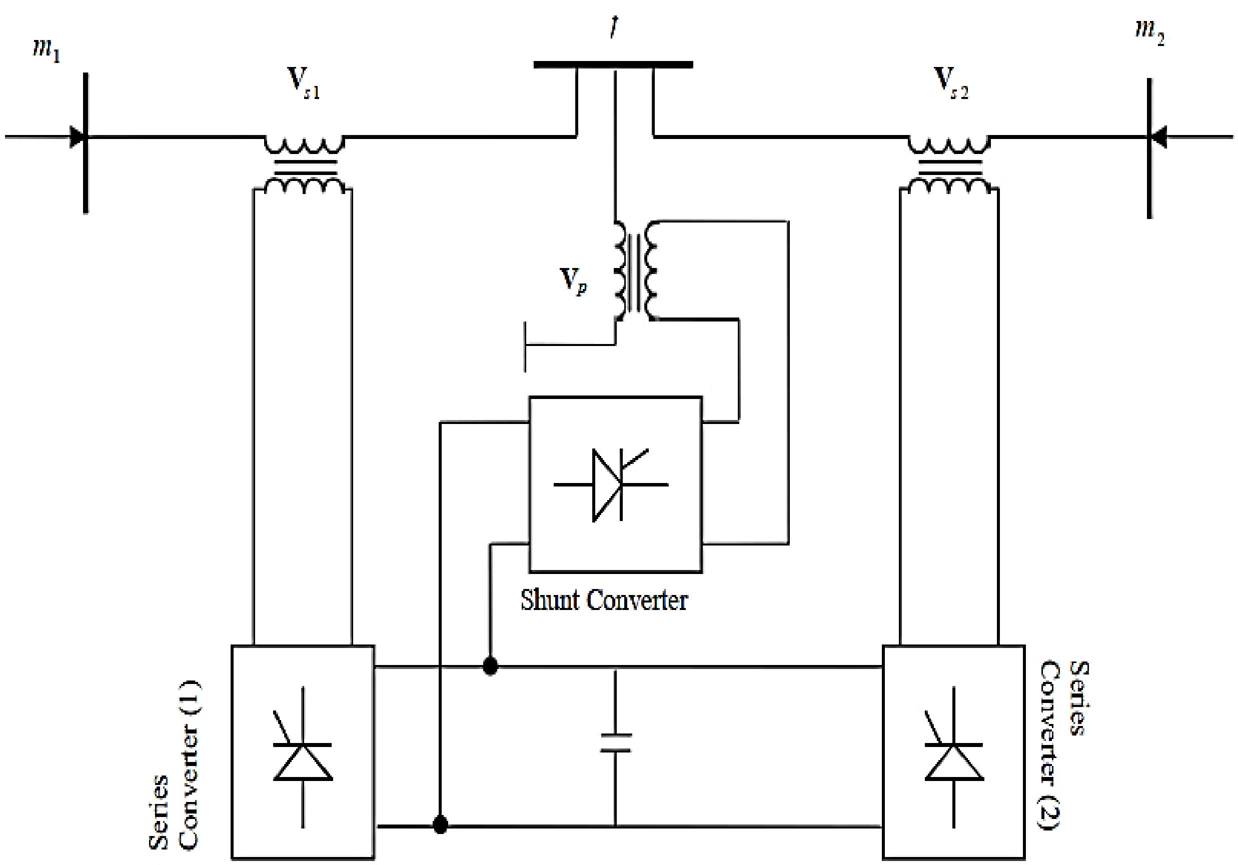

Figure 2.4: Simplified model of GUPFC

On the other hand, the GUPFC consists of three converters, one connected in shunt and the other two in series with two transmission lines in a substation in order to control bus voltage and power flows of more than one line by referring to the figure 2.4. The series controllers can be two SSSCs, while STATCOMs can be used as the shunt controllers.

Table 2.1: Comparison between conventional and major FACTS devices.

Item	Conventional (Switched)	FACTS Devices (Fast, static)	
Technology	Resistance, inductance or capacitance together with transformers which are fixed or mechanically switched	Resistance, inductance or capacitance together with transformers which are switched in smaller steps or with switching patterns within a cycle of the alternating current by using additional power electronic valves or converters.	
Main components	R, L, C, Transformer	Thyristor valve	VSC
Shunt Devices	Switched-Shunt Compensation (L, C)	SVC	STATCOM
Series Devices	(Switched) Series Compensation (L, C)	TCSC / TPSC	SSSC
Shunt - Series Devices	PST	DPFC	UPFC/ IPFC

By referring to table 2.1, a brief overview of the major conventional and FACTS controllers and the associated categories have described. In this section, PST was found as traditionally used device to control the active power by reducing the power flow on overloaded lines while redirecting the power to flow on lines with free capacity. But the reactive power consumption by PSTs is unacceptable and PSTs have limited speed of control. UPFC is a versatile device that can control various system variables independently and its application to solve congestion problems in an actual grid. However, the capital cost of this controller is a major obstacle for the wide application of this technology in power systems [19].

Finally, the above table also shows that both STATCOM and SSSC use VSC technology to allow high modulation frequencies and thus, low output harmonics but with increased powers losses.

2.2.3. STATIC SYNCHRONOUS COMPENSATOR (STATCOM)

a. Definition and application

STATCOM is shunt connected devices whose primary role is to control transmission voltage by reactive power shunt compensation and can improve the power quality. against even dips and flickers. It uses GTOs or IGBT technology which provides smoother and more precise control one step further than commonly used SVC.

b. Architecture and operation

A typical STATCOM consists of a coupling transformer, an inverter (VSC) and a DC capacitor. A VSC is a device which converts DC to AC whereby the AC output control is achieved by the use of electronic switching devices like IGBT or GTO for lower and higher power respectively.

DC capacitor stores energy at the interface between the electrode and electrolyte whereby the application of a voltage causes the flow of the ions.

The STATCOM controls the reactive power by the means of changing output voltage which is generated by VSC. If the VSC output voltage is higher than the grid voltage, the STATCOM acts as a capacitor to generate the reactive power to the grid. If the VSC output voltage is less than the grid voltage, the STATCOM acts as a reactor to absorb the reactive power from the grid. As previously explained, the STATCOM contains a coupling transformer, VSC and DC energy storage. Figure 2.5 shows the basic structure and characteristics of the STACOM controller.

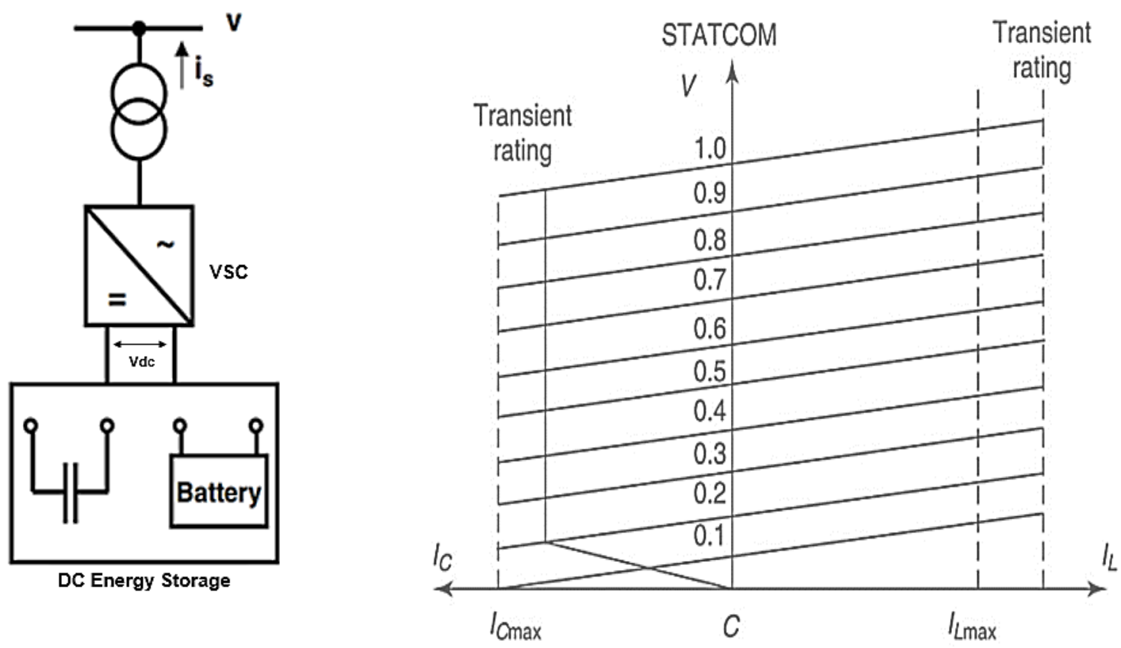

(a) Basic structure of STATCOM (b) V-I characteristics of STATCOM

Figure 2.5: Basic structure and characteristics of STATCOM

From the figure 5, the following equations can be found:

$$I = \frac{V - E}{X}$$

Whereby, E, V, X and I are the injected VSC voltage, line voltage, coupling transformer and inverter reactance, and the injected current into a transmission line respectively. Therefore, the compensated reactive power becomes:

$$Q = IV = \frac{V - E}{X} V = \frac{1 - \frac{E}{V}}{X} V^2$$

Thus,

- If $E > V$, the reactive power flow from the controller to the grid, the system becomes over-excited.
- If $E < V$, the reactive power flow from the grid to the controller and the system becomes under-excited system.

In this study, it is assumed that both the active power exchange between the AC system and the STATCOM and the harmonics which can be generated by the STATCOM are neglected.

c. Control scheme

The reactive power can be exchanged between the STATCOM and the grid by changing the output voltage of the converter. If the amplitude of the output voltage is increased above that of the system bus voltage, the current flows through the reactance from the converter to the system and the converter generates capacitive-reactive power for the system. Otherwise, if the amplitude of the output voltage is decreased below the bus voltage, the current flows from the system bus to the converter and consequently, the reactive power is absorbed by the converter from the system. If the STATCOM voltage equals the AC system voltage, there is no reactive-power exchange.

The STATCOM is controlled by setting the required active and reactive power for reference as shown in figure 2.6 and 2.7.

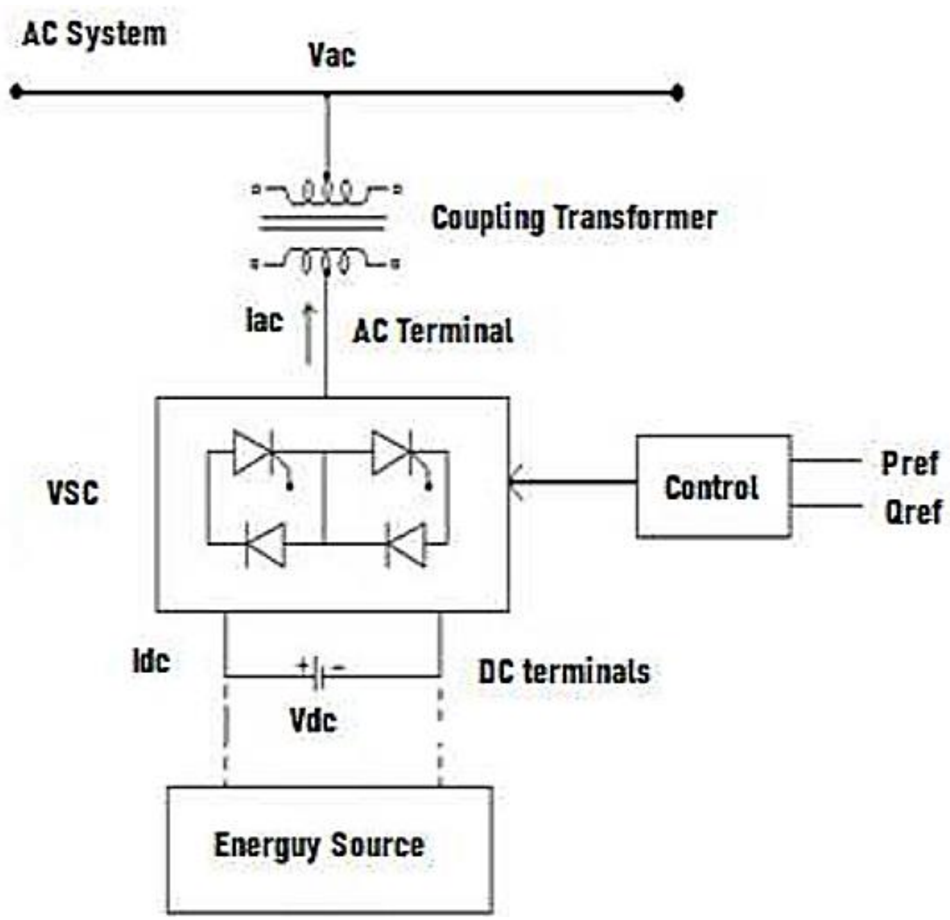

Figure 2.6: Basic diagram for the controlled STATCOM [8]

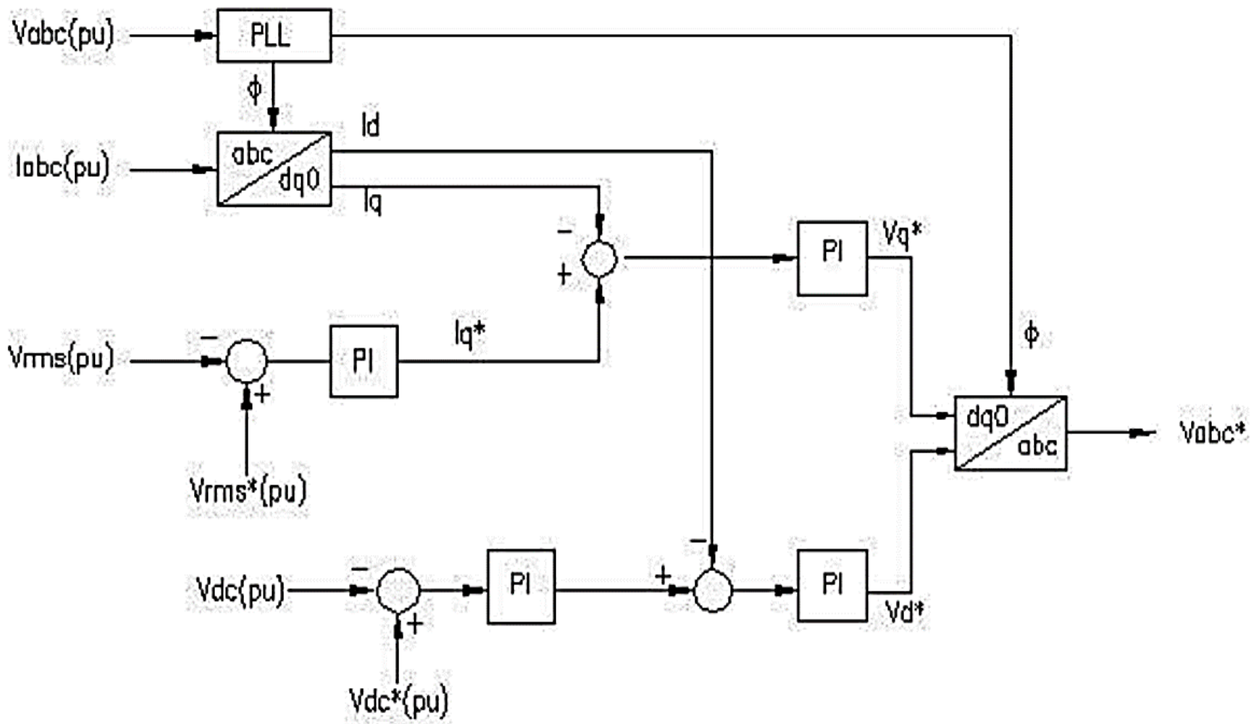

Figure 2.7: Control scheme of STATCOM

In fact, the control system consists of:

- A PLL is an electronic control circuit which produces an output period signal whose phase is related to the phase of an input signal. In fact, PLL is composed of a variable frequency oscillator which generates signal and the phase detector to make a comparison of the phase signal and oscillator's signal in order to keep both phases in line. During the PLL operations, the angle φ is transformed to the abc to $dq0$ and $dq0$ to abc. The first PI controller controls the terminal voltage by exchanging the reactive power with the AC system. The output of PI regulator is the reactive current reference I_q^*, which is limited with $\pm 1pu$ as either capacitive or inductive current respectively. The second PI regulator serves to maintain DC voltage constant by letting the active power exchange with the AC network, the compensation of the active power losses in the transformer and converter. It produces I_d^* as active current reference. The two remaining PI regulators provides the reference voltage V_d^* and V_q^* to the PWM signal generator of the converter after a $dq0$ to abc transformation. As result, the output three phase voltages is generated as V_{abc}^* from the converter output.

- Measurement systems measure the q −components of AC positive sequence of voltage V_{1q} and V_{2q}) as well as the DC voltage V_{dc}. AC and DC voltage regulators which compute the two components of the required converter voltage (V_{d_conv} and V_{q_conv}) to obtain the desired DC voltage (V_{dcref}) and the injected voltage (V_{qref}). The V_q voltage regulator is assisted by a feed forward type regulator which predicts the V_conv voltage from the I_d current measurement.
- PI controller is a proportional gain in parallel with an integrator, both in series with controller. The Proportional gain provides fast response. The integrator drives the system to 0 steady-state error.

2.2.4. STATIC SYNCHRONOUS SERIES COMPENSATOR (SSSC)

a. Definition and application

SSSC is series compensated device which uses the DC energy storage to exchange reactive power along with AC system by influencing the effective impedance in the line and hence, they can support the reactive power compensation as shown in the below figure 8.

It comprises the synchronous source of voltage (VSC GTO based inverter), a coupling series transformer and a DC capacitor like STATCOM to produce three phase supply voltage, that are further injected to transmission line.

b. Architecture and operation

In fact, SSSC uses electronic switches which inject quadrant voltage lagging the current in the line. The operation of SSSC is displayed in figure 2.8. The SSSC injects a variable output voltage is in quadrature (90º leading or lagging) with, and controllable independently of the line current for the purpose of increasing or decreasing the overall reactive voltage drop across the line and thereby controlling the transmitted electric power. When the line current leads the voltage by 90 degrees, it works as series capacitor, and it imitates a series inductor when current is lagging by 90 degrees.

The impedance is controlled by controlling switch voltage which is proportional to the current. By inversing switch output voltage, the line impedance will be increased, thus limiting the fault current or power reduction. Furthermore, it is more advanced than TCSC because it does not harmonics in the network. In normal practices, the power transfer is constrained by a load factor (of 60% approx.), voltage constraint (Line voltage is 95% of source voltage) and transient stability limits (for stable system, phase angle at 2-line extremities is supposed to be less than 35°).

Therefore, SSSC can provide the following solutions in the network.

a. Modification of load curve by use of load management methods,
b. Modification of the line characteristics by use of FACTS. $P_e = \frac{V_1 V_2}{X} sin\delta$ whereby Pe is the transmitted power, V_1 and V_2 are the voltage amplitudes at line extremities; δ is the phase angle between V_1 and V_2 and X is line impedance. In this case, the losses are assumed to be negligible. Therefore, FACTS can regulate power through controlling one, two or three of V, X and δ.
c. Line control with FACTS.
d. The use of STATCOM to modify load curve, active and reactive power control, and improvement of transient stability by use of line control.

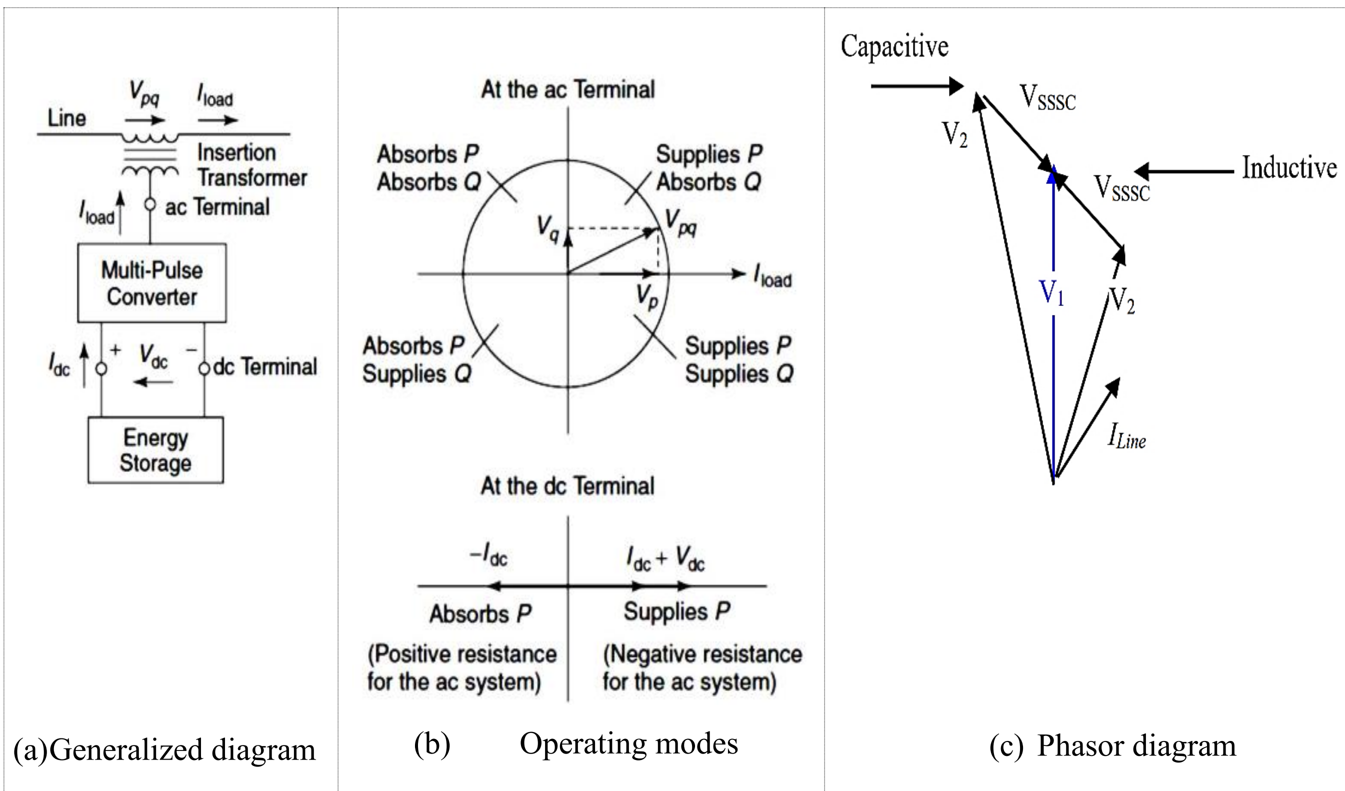

Figure 2.8: Generalized diagram and the power exchange for SSSC

c. Control scheme

The control system consists of:

- A PLL synchronizes on the positive-sequence component of the current I whereby its output is given as the angle $\theta = \omega t$ to calculate the direct-axis and quadrature-axis components of the AC three-phase voltages and currents as V_d, V_q, I_d and I_q on the figure 2.9.
- Measurement systems help to measure the q components of AC positive sequence of voltages V_1 and V_2 (V_{1q} and V_{2q}) as well as the DC voltage V_{dc}.
- AC and DC voltage regulators computes the two components of the required converter voltage (V_{d_conv} and V_{q_conv}) to obtain the desired DC voltage (V_{dcref}) and the injected voltage (V_{qref}). The V_q voltage regulator is assisted by a feed forward type regulator which predicts the V_{conv} voltage from the I_d current measurement.
- PI controller has a proportional gain in parallel with an integrator, both in series with controller. The Proportional gain provides fast response. The integrator drives the system to a 0 steady-state error. PI controller is one of the most widely sought after controllers in industry as it is the simplest to design.

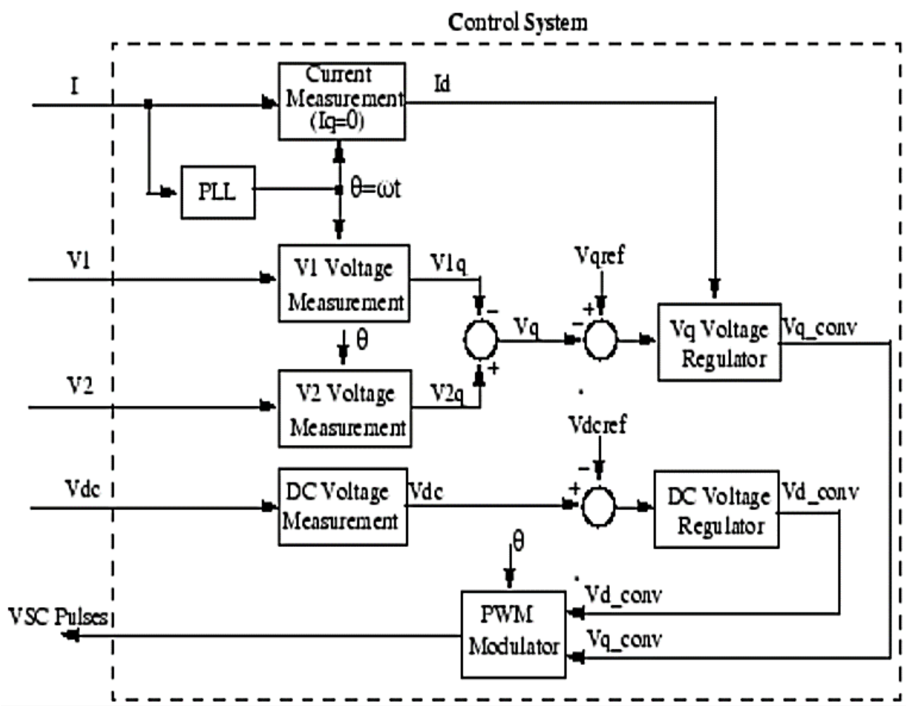

Figure 2.9: Control Scheme of SSSC

The active and reactive power of the bus is calculated using their voltage and current in dq0 references and compared with the determined reference and the produced error signal is given to the PI controllers. We adjust the parameters of PI controller, trying to achieve zero signal error, so that power can follow through the reference powers precisely. Then the output of the controllers are transformed to abc reference voltage and given to the PWM [12].

2.3.EXISTING HIGH VOLTAGE POWER NETWORK IN KIGALI ZONE

2.3.1. EXISTING NETWORK

The existing electrical power grid comprises the generation plants and substations which are interconnected to the electricity users by the means of power lines with different levels of voltages: 0.4kV or 0.2kV for LV systems, 6.6kV, 11kV, 15kV or 30kV for MV systems and 110kV and 220kV for HV systems as per the map in the figure 10. The actual transmission network is characterized by different perspectives as per table 2.2.

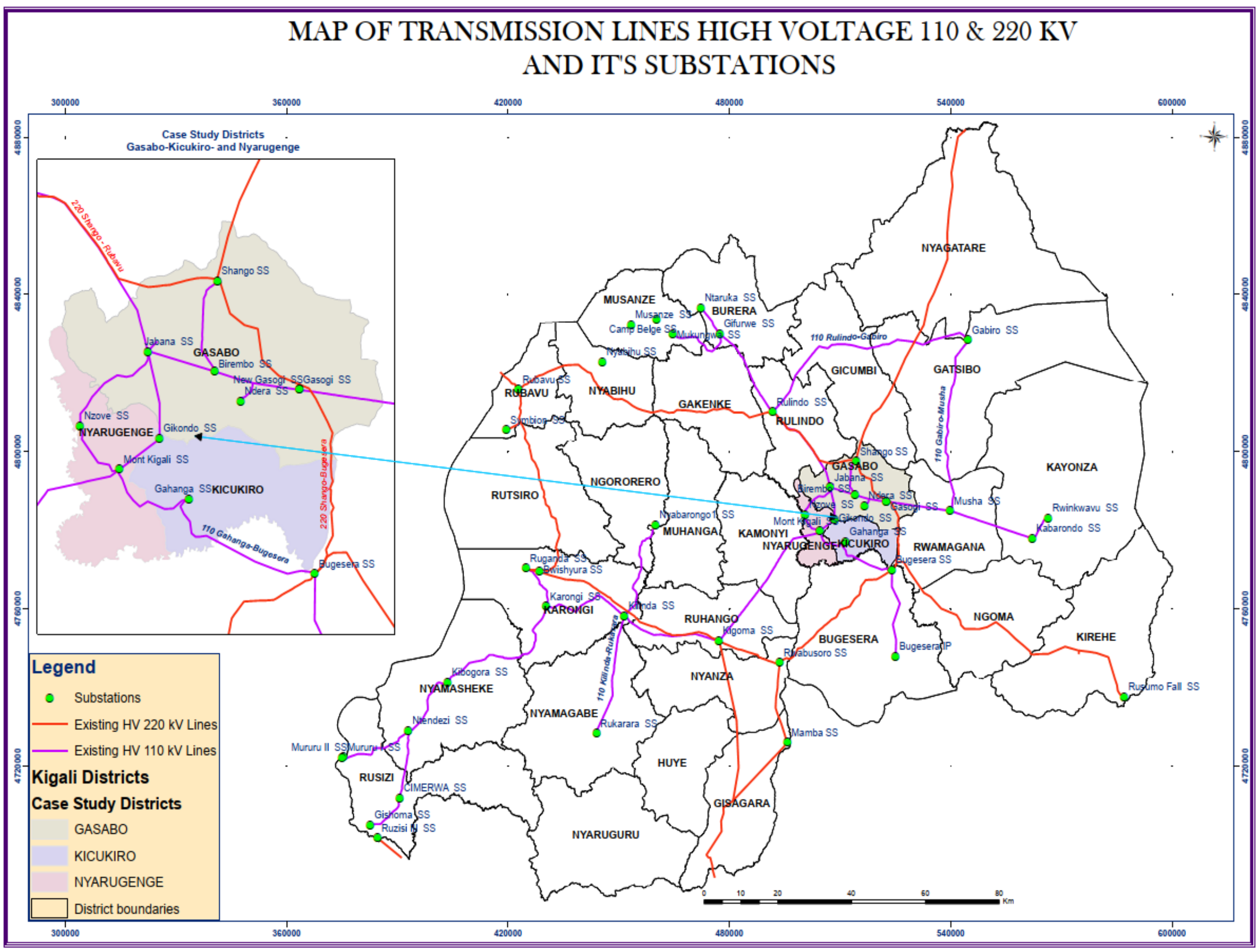

Figure 2.10: Map of HV transmission lines and substations

Table 2.2: Grid expansion with the associated financial losses during the last three FYs

Network category	Description		Details		
			FY 2019-2020 [20]	FY 2020-2021 [21]	FY 2021-2022 [1]
Generation systems	Hydropower		94.678 MW	104.628 MW	107.328 MW
	Thermal Power		58.8 MW	58.8 MW	58.8 MW
	Solar Power		12.05 MW	12.05 MW	12.05 MW
	Methane Gas		29.79 MW	29.79 MW	29.79 MW
	Import & Shared		18.1 MW	18.1 MW	18.1 MW
	Peat Fired Power Plant		15 MW	15 MW	50 MW
	Total installed capacity in MW		**228.418**	**238.368**	**276.068**
Transmission systems	Total length of HV lines		-	944.39 km	973.14 km
	Number of main substations		-	37	37
	Financial losses from power quality disturbances in Rwf	Undervoltage	36,291	-	-
		Overvoltage	16,989,246	932,914	-
		Underfrequency	56,842,910	77,847,070	86,202,751
		Overload	6,023,449	2,908,428	877,623
		Total	**79,891,896**	**81,688,412**	**87,080,374**
Distribution systems	Total length of MV lines in km		412	738.5	10,520.1
	Total length of LV lines in km		856	1,280.7	18,465.7
Utilization systems	Highest peak demand in MW		151.02	164.4	178.71

Table 2.3: Major network instability problems per year [1], [20], [21] [22].

Item	UoM	FY 2015-2016	FY 2016-2017	FY 2017-2018	FY 2018-2019	FY 2019-2020	FY 2020-2021	FY 2021-2022
Blackouts	Nos	35	21	20	3	5	1	4
Power Losses	%	22.70	21.08	19.82	19.39	19.12	19.26	18.10

The table 2.2 also displayed the recent situation whereby the national grid was suffered with different power quality disturbances including the undervoltage, overvoltage, under frequency overload which were contributed to the financial loss of 79,891,896 Rwf, 81,688,412 Rwf and 87,080,374 Rwf in FY 2019-2020, FY 2020-2021 and FY 2021-2022 respectively. REG has also recorded the different levels of power losses and blackouts as per table 2.3.

On the other hand, the HV network in Kigali zone under our study comprises:

i. Three power plants such as Jabana 1, Birembo and Masoro Thermal Power plants.
ii. Ten step-down substations such as Jabana 2, Nzove, Mont Kigali, Gikondo, Gahanga, Rilima, Shango, Birembo, Ndera and Gasogi and their associated transmission lines.
iii. Five power supplies from upcountry power plants like Northern, North-Western, South-Western, South-Eastern and Eastern gates, and,
iv. The reactive power compensators such as shunt capacitor banks which are installed at the MV side of Jabana, Birembo and Gikondo substations with the capacity of 3x1.5Mvars per each substation in addition to three shunt reactors which are installed at Rilima, and Shango substations.

2.3.2. FUTURE NETWORK

The estimation of the future development is based on the information which were received from REG during September 2023, and they include previous feasibility studies for the transmission network. In fact, the future network will be characterized by the increased generation capacity and electricity demand with their corresponding network extensions. The previous studies shows that Rwanda has the electricity generation reserves with 443.6 MW, and it can be expected the highest peak load can reach be 463.53 MW [23].

The Lagrange extrapolation formula helps to forecast the expected financial losses are estimated to reach 26,020,224,615 Rwf in 2032 if no immediate action is taken. The figure is calculated by the use of data from the last three year (2020, 2021 and 2022) and the extrapolation equations:

$$P_2(x) = y_0 l_0(x) + y_1 l_1(x) + y_2 l_2(x)$$

Whereby

- x_i is number of years i.
- y stands for financial losses.

- l_i, is the Lagrange factor which correspond on the previous year i.

In our case, $x_0 = 2020$, $x_1 = 2021$ and $x_2 = 2022$,

$$l_0(x) = \frac{(x - x_1)(x - x_2)}{(x_0 - x_1)(x_0 - x_2)};\ l_1(x) = \frac{(x - x_0)(x - x_2)}{(x_1 - x_0)(x_1 - x_2)};\ l_2(x) = \frac{(x - x_0)(x - x_1)}{(x_2 - x_0)(x_2 - x_1)}$$

Therefore, the calculation results show that the financial losses in the year of 2032 will be 55 times the current losses (2022), which will be a huge burden to the utility company.

In addition, the loads have been modelled by assuming the trending load which increases at uniform rate of 10% which will always increase proportionally with the population growth until 2032. This basis of estimation is in line with the methodology which was used by IEC Generation System Planning Department. According to the National power Master Plan for Rwanda, the load has been forecasted by IEC Generation System Planning Department and the used algorithm was approved by REG, and therefore the findings are shown in table 2.4. Also, the future generation is estimated by based on the development plans whereby the table 6 shows the expected generation. Also, table 2.5 gives the total future generation versus demand.

Table 2.4: Forecasted load [24]

Year	Peak load in MW with 8% growth rate	Peak load in MW with 10% growth rate	Peak load in MW with 12% growth rate
2016	119	119	119
2017	129	131	133
2020	162	174	187
2025	238	281	330
2030	350	452	582

Table 2.5: Future generation

No	Power plants	Type	Generation capacity
1.	Nyabarongo 2	Hydropower	37 MW
2.	Rukarara 6	Hydropower	6.7 MW
3.	Rusumo Falls	Imported Hydropower	26.7 MW
4.	Rusizi 3	Imported Hydropower	48.3 MW
5.	Extension of KIVUWATT	Methane Gas to Power	8 MW
6.	Hakan	Peat to Power	35 MW
7.	Bihingore	Hydropower	5.35 MW
Total			167.05MW

The table 2.6, shows that the future national network will not be stable, and it requires extra effort to fulfill the load requirements. Therefore, one of the alternative sustainable solutions is to review the proper operation to schedule the HV network by integrating the powerful FACTS controllers to avoid the voltage collapse which may occur especially in Kigali Zone.

Table 2.6: The electricity generation and demand in the year 2032 according to the region

Region	**Future generation [MW]**		**Peak Demand [MW]**	
	Existing	Expected	Existing	Expected
Kigali	101.89	113.14	123.98	292.34
South-West	78.42	170.42	41.2	80.6
South-East	35	75	14.75	34.78
East	11.8	11.8	30	75.3
North-West	73.232	68.582	30	70.8
Total	300.342	438.942	239.93	553.82
Future balance (Expected generation – Expected peak demand) = -114.878 MW				

CHAPTER 3. METHODOLOGY

This chapter describes a set of procedures which have been followed in order to reach the expected results of the research.

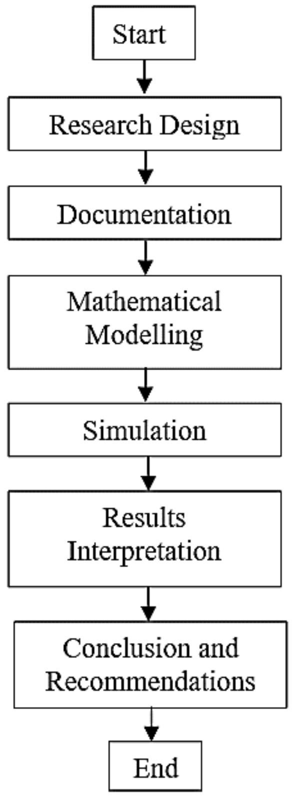

Figure 3.1: Research methodology

3.1.RESEARCH DESIGN AND DOCUMENTATION

During the research design, all strategies, rules, tools, data, timelines, and limitations which have been identified to guide this research from its conception to the conclusion. Initially, the UR requirements and guidelines have been accessed on the university website link https://ur.ac.rw/documents/academics/GUIDELINES%20ON%20ACADEMIC%20WRITING.pdf in order to ensure an effective writing of a successful dissertation.

The review of the existing studies took place in order to understand and confirm the architecture and operating characteristics of the Rwandan electric grid along with its associated problems. On the other hand, the available online resources in terms of reports, books, papers, journals and standards have been accessed, read, downloaded, and filed into hard disk to have a deeper understanding of electrical systems, theories, practices and software tools which will be required to obtain the optimistic research outcomes.

As result, the following deliverables have been identified:

- Rwanda Energy Group and its subsidiaries (EDCL and EUCL) as provider of data which are related to the Rwandan electrical network.
- Lagrange model as a forecasting method for the future financial losses from outages.
- Newton Raphson Method, to model the power system mathematically.
- Convenient software such as Matlab/Simulink to perform and simulate the proposed model; Microsoft office for dissertation writing and Mendeley for referencing,

3.2.MATHEMATICAL MODELING

- **Lagrange's method**

This Lagrange's method has been used in section 2.3.2 of this research report in order to model and calculate the future financial losses from the network disturbances if there are no mitigation measures taken at the moment. The Lagrange's method states that for any such set of data, there is an n-degree polynomial that interpolates it. In this regard, the interpolating polynomial becomes:

$$p_n(x) = \sum_{i=0}^{n} y_i l_i(x) \qquad 3.1$$

$$l_i(x) = \prod_{j=0, j\neq i}^{n} \frac{x-x_j}{x_i-x_j} \qquad 3.2$$

such that $p(x_i) = y_1$ for $i = (0; \ldots\ldots; n)$

- **Newton Raphson Method**

This is the iterative Newton method to solve the non-linear matrix equations of large dimension. In normal practices, the network can be analyzed by using different methods including but not limited to the nodal and loop analysis. Unfortunately, the conventional nodal or loop analysis is not suitable for power-flow studies because the input data for loads are normally given in terms of power, not impedance. Also, generators are considered as power sources, not voltage or current.

Since the power networks are non-linear systems, the Newton-Raphson method is necessary and used to calculate the real and reactive power flow from generators to loads at every point of a transmission line, along with the associated bus voltages.

The method states that let y and x are N vectors and $f(x)$ is an N vector of functions. The y and $f(x)$ are given as per the equation 3.3 in order to solve for x.

$$f(x) = \begin{bmatrix} f_1(x) \\ f_2(x) \\ \vdots \\ f_N(x) \end{bmatrix} = y \qquad 3.3$$

The Newton Raphson method thus gives:

$$x(i+1) = x(i) + J^{-1}(i)\{y - f[x(i)]\} \qquad 3.4$$

$J(i)$ is Jacobian matrix and calculated as per equation 3.5.

$$J(i) = \left.\frac{df}{dx}\right|_{x=x(i)} = \begin{bmatrix} \frac{\partial f_1}{\partial x_1} & \frac{\partial f_1}{\partial x_2} & \cdots & \frac{\partial f_1}{\partial x_N} \\ \frac{\partial f_2}{\partial x_1} & \frac{\partial f_2}{\partial x_2} & \cdots & \frac{\partial f_2}{\partial x_N} \\ \vdots & \vdots & \ddots & \vdots \\ \frac{\partial f_N}{\partial x_1} & \frac{\partial f_N}{\partial x_2} & \cdots & \frac{\partial f_N}{\partial x_N} \end{bmatrix}_{x=x(i)} \qquad 3.5$$

Finally, the equation 3.4 becomes equivalent to the equation 3.6.

$$J(i)\Delta x(i) = \Delta y(i) \qquad 3.6$$

Whereby, $\Delta x(i) = x(i+1) - x(i)$ and $\Delta y(i) = y - f[x(i)]$

i and $i+1$ are the current and the next iteration respectively.

In general, during each alteration, the following steps should be completed to solve any non-linear equation:

1. Compute $\Delta y(i) = y - f[x(i)]$
2. Compute

$$J(i) = \left.\frac{df}{dx}\right|_{x=x(i)} = \begin{bmatrix} \frac{\partial f_1}{\partial x_1} & \frac{\partial f_1}{\partial x_2} & \cdots & \frac{\partial f_1}{\partial x_N} \\ \frac{\partial f_2}{\partial x_1} & \frac{\partial f_2}{\partial x_2} & \cdots & \frac{\partial f_2}{\partial x_N} \\ \vdots & \vdots & \ddots & \vdots \\ \frac{\partial f_N}{\partial x_1} & \frac{\partial f_N}{\partial x_2} & \cdots & \frac{\partial f_N}{\partial x_N} \end{bmatrix}_{x=x(i)}$$

3. Solve for $\Delta x(i)$ from $J(i)\Delta x(i) = \Delta y(i)$
4. Compute $x(i+1)$ from $\Delta x(i) = x(i+1) - x(i)$

3.3.DATA COLLECTION

The relevant queries have been formulated and discussed in detail, the template and types of data to be collected have been prepared prior to the performance of data collection and after reviewing the features of the simulation software. And, thus, the request for facilitation in data collection has been sent to EDCL, the subsidiary of REG. Appendix 1 thus displays EDCL acceptance to facilitate in data collection whereas the Table 3.1 shows survey forms to be filled with the network data at each 110kV and 220kV busbar in Kigali.

Table 3.1 Types of surveyed data

Item	Purpose	Data type
Generation plant	To estimate the total generation capacity (Current and future) to supply Kigali HV network	1. Power Plant name 2. Type of power plant 3. Location of power plant 4. Generation capacity
Load demand at each HV bus from 2020, 2021 and 2023	To estimate the current and future total load requirements countrywide.	1. Substation bus name 2. Voltage level 3. Active power 4. Reactive power 5. Location of substation bus 6. Bus capacity
HV Transformers	To estimate the transformer performance and associated losses on power flow in terms of resistances, reactance or impedance.	1. Transformer name 2. Location 3. Status (In service or not) 4. Transformer apparent power rating 5. Transformation ratio 6. Magnetizing 7. Losses (No-load, load, flux, and eddy Current) 8. Load losses
HV transmission lines	To estimate the transmission line performance and associated technical losses on power flow	1. Transformer name 2. Location 3. Line length 4. Voltage level 5. Rated apparent power. 6. Positive and zero-sequence impedance

On the appendices 2, 3, 4 and 5 provide the details for the obtained data from REG.

3.4.SIMULATION USING MATLAB/SIMULINK

All simulations of power generation plants, demand, transmission lines, transformers, STATCOM and SSS have been done in this study with the help of Simulink® block diagram environment.

In fact, Simulink® block diagram environment is integrated with MATLAB® 2017a to facilitate the performance of different designs and simulations of a model as well as dynamic systems. It is used in this study to investigate and analyze the existing and future power transmission network stability. The below steps have been followed to get end result within the Simulink:

(a) System modelling, whereby the equivalent circuit of any equipment is modelled by using block diagrams.
(b) Input data, whereby all surveyed characteristic parameters are registered and assigned to each power system component such as a generation plant, bus, transformer, lines, load as well as FACTS controllers.
(c) Generation of simulation outputs, whereby the simulation results are displayed at each component in terms of active power, reactive power, phase angle, voltage, current, impedances and their associated waveforms.

3.5.RESULTS INTERPRETATION

This is the last step to visualize the voltage stability in case of network disturbances. The voltage variations in the simulated future network with FACTS devices will be compared with the existing network voltages to showcase the improvement. Basically, the voltage failure arose when system is overloaded yonder its extreme load capability point [8]. The capability limits at the point of connection are shown in the table 3.2 according to Rwanda electricity grid code and the figure 3.2 as per IEC 60034-3 [25].

Table 3.2: Steady state voltage conditions at transmission buses

No	Conditions	Steady State Voltage Range
a.	Under normal conditions	$0.95\ pu \leq V_{bus} < 1.05\ pu$
b.	Under any single contingency	$0.90\ pu \leq V_{bus} < 1.10\ pu$
c.	Multiple contingency	$0.85\ pu \leq V_{bus} < 1.20\ pu$

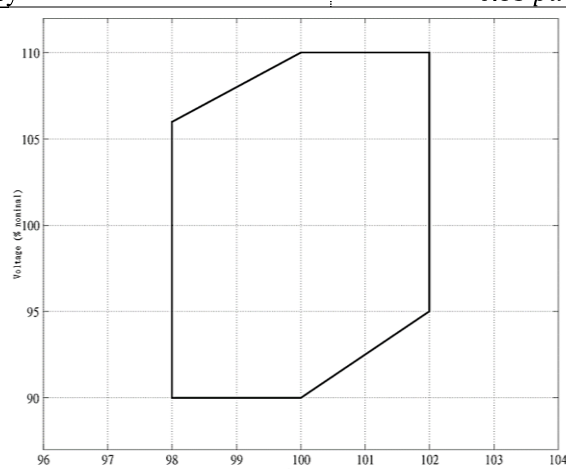

Figure 3.2: Frequency-voltage tolerances required from Unit at the Point of Connection[25]

CHAPTER 4. MODELLING AND SIMULATION OF HIGH VOLTAGE NETWORK WITH STATCOM AND SSSC CONTROLLERS

4.1.OVERVIEW

The power flow calculation is one of the most fundamental components in the analysis of power systems and is the cornerstone for almost other tool used in power systems simulation and management [13].

Due to a limited time, it is difficult to model the entire power network. Therefore, this section focused on the analysis of Kigali HV network by breaking the national grid into 5 zones such as Kigali, South-Western, South-Eastern, West-Northern, and Eastern. The zones which are out of Kigali have been replaced by the equivalent model in terms of generation and demand with some reasonable assumptions.

4.2.MATHEMATICAL MODELLING OF KIGALI HIGH VOLTAGE NETWORK

As described in chapter 3, the Newton Raphson Method is used as mathematical tool to model and solve power flow problem, especially for Kigali HV network.

First all, it was assumed that the power system is balanced, whereby three phases are symmetrical to each order, and consequently, it has allowed to analyze one phase only instead of three phase to reduce number of equations. The figure 4.1 thsu shows general power flow layout at any given system.

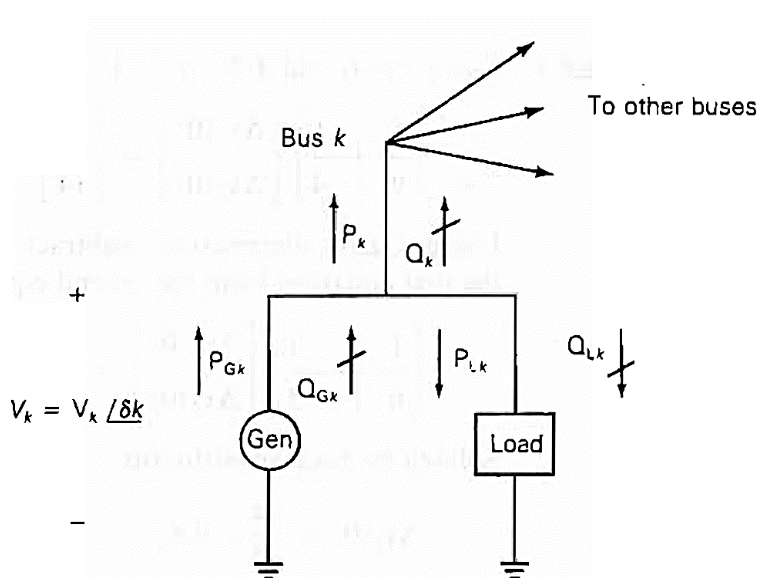

Figure 4.1: Power flow of any given system

Let V_k, δ_k, P_k and Q_k, be therefore voltage magnitude, phase angle, net real power, net reactive power at each bus k respectively as bus variables. The two of them are always specified whereas the other two are unknown at each bus and to be computed by power flow program. According to the above definition and shown in figure 14, the active and reactive power flow from bus k to other buses can be calculated by using Kirchhoff law to get the equations 4.1 and 4.2.

$$P_k = P_{Gk} - P_{Lk} \quad 4.1$$

$$Q_k = Q_{Gk} - Q_{Lk} \quad 4.2$$

Whereas P_{Gk}, Q_{Gk}, P_{Lk} and Q_{Lk} are generated active power, generated reactive power, consumed active power, and consumed reactive power at any bus k respectively.

In fact, Kigali HV network as a case study has two 220kV buses and ten 110kV buses. The active and reactive power are generated to Kigali network from West-Southern region through 110kV Mont Kigali bus, West-Northern region through 110kV Jabana 2 bus, West-Northern region through 220kV Shango bus, East-Southern region through 220kV Rilima bus and Eastern region through 110kV Gasogi bus. There are also thermal power plants in Kigali region at Birembo, Masoro and Jabana (1 and 2) which supply the electrical power through 110kV Birembo, Ndera and Jabana 2 buses respectively. Figure 4.2 displays the interconnection layout of generation plants, buses, transformers, transmission lines, and their associated load in Kigali HV network.

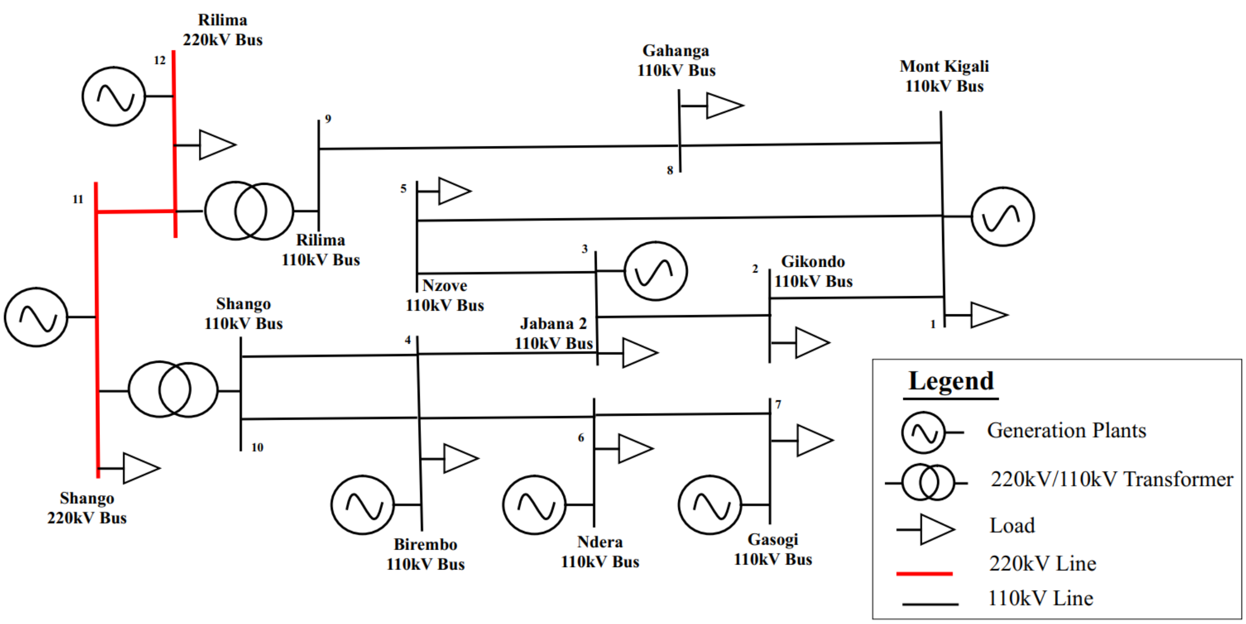

Figure 4.2: Single line diagram of Kigali HV network

4.2.1. POWER FLOW MODEL AT ANY SYSTEM BUS

The total real and reactive power of all N buses can be found by using the equation 4.3 and 4.4.

$$P_{T,k} = \sum_{i=1}^{N} V_k V_i Y_{i,k} cos(\beta_k - \beta_i - \vartheta_{i,k}) \quad 4.3$$

$$Q_{T,k} = \sum_{i=1}^{N} V_i V_k Y_{i,k} sin(\beta_k - \beta_i - \vartheta_{i,k}) \quad 4.4$$

Whereby, $k = 1,2,3,4, \dots N$; $Y_{i,k}$ stands for the admittance between i^{th} and k^{th} buses and $\vartheta_{i,k}$: Angle on $Y_{i,k}$ admittance. As well, $N = 12$ in order to mean that Kigali network has 12 HV buses as per research case study.

The total active power flow, $P_{G,k} - P_{L,k}$ at any bus k can be obtained as per the equation 4.6 by substituting equation (4.3) in (4.1).

$$P_{G,k} = P_{L,k} + \sum_{i=1}^{N} V_k V_i Y_{i,k} cos(\beta_k - \beta_i - \vartheta_{i,k}) \quad 4.5$$

$$P_{G,k} - P_{L,k} - \sum_{i=1}^{N} V_k V_i Y_{i,k} cos(\beta_k - \beta_i - \vartheta_{i,k}) = P_k(V, \beta) = P_k = 0 \quad 4.6$$

On the other hand, the total reactive power flow, $Q_{G,k} - Q_{L,k}$ at any bus k can be obtained as per the equation 4.8 by substituting equation (4.4) in (4.2).

$$Q_{G,k} = Q_{L,k} + \sum_{i=1}^{N} V_i V_k Y_{i,k} sin(\beta_k - \beta_i - \vartheta_{i,k}) \quad 4.7$$

$$Q_{G,k} - Q_{L,k} - \sum_{i=1}^{N} V_i V_k Y_{i,k} sin(\beta_k - \beta_i - \vartheta_{i,k}) = Q_k(V, \beta) = Q_k = 0 \quad 4.8$$

In this case, the Newton Raphson method can be used to find the admittances.

4.2.2. TRANSFORMER AND TRANSMISSION LINE MODELS

A transmission line has been modelled from its equivalent π circuit in figure 4.3, which is composed of the series impedance $Z = R + jX$ and the shunt admittance $Y_{sh} = jB_c$ between two buses (S and R) to which the line is connected.

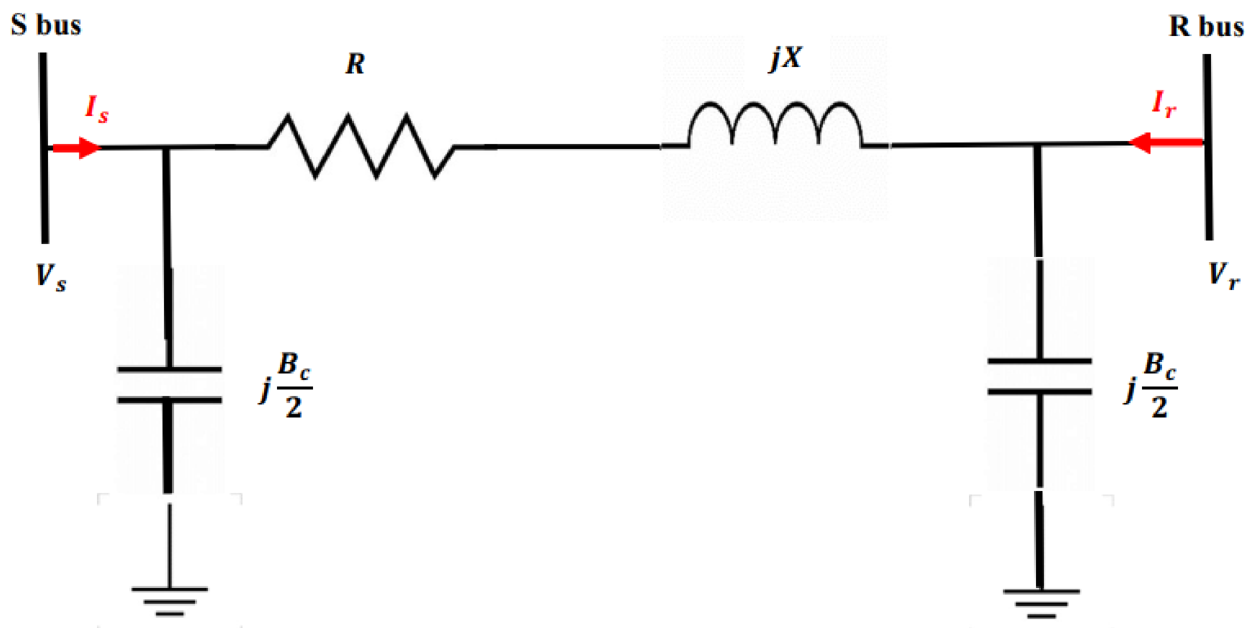

Figure 4.3: Equivalent π circuit of a transmission line

The equivalent two-port equations 4.9 and 4.10 therefore show the relationship between sending and receiving ends voltages and currents.

$$\begin{bmatrix} V_s \\ I_s \end{bmatrix} = \begin{bmatrix} 1 + j\frac{B_c}{2}Z & Z \\ j\frac{B_c}{2}(2 + j\frac{B_c}{2}Z) & 1 + j\frac{B_c}{2}Z \end{bmatrix} \begin{bmatrix} V_r \\ I_r \end{bmatrix} \quad 4.9$$

$$\begin{bmatrix} I_s \\ I_r \end{bmatrix} = \begin{bmatrix} Y + j\frac{B_c}{2} & -Y \\ -Y & Y + j\frac{B_c}{2} \end{bmatrix} \begin{bmatrix} V_s \\ V_r \end{bmatrix} = \begin{bmatrix} Y_{ss} & Y_{sr} \\ Y_{rs} & Y_{ss} \end{bmatrix} \begin{bmatrix} V_s \\ V_r \end{bmatrix} \quad 4.10$$

Whereby, $V_s = V_s\angle\delta_s$, $V_r = V_r\angle\delta_r$, $Z = R + jX$, $Y = \frac{1}{Z}$, $Y_{ss} = Y_{rr} = G_{ss} + jB_{ss} = Y + j\frac{B_c}{2}$, and $Y_{sr} = Y_{rs} = G_{sr} + jB_{sr} = -Y$.

Therefore, the apparent powers S_s and S_r which are injected to the buses S and R are given in the in the equations respectively.

$$S_s = V_s I_s^* = V_s(Y_{ss}V_s + Y_{sr}V_r)^* \quad 4.11$$

$$S_r = V_r I_r^* = V_r(Y_{rs}V_r + Y_{rr}V_r)^* \quad 4.12$$

And the injected real and reactive power flow to the buses S and R are found as:

$$P_s = G_{ss}V_s^{\ 2} + (G_{sr}\cos\delta_{sr} + B_{sr}\sin\delta_{sr})V_sV_r \qquad 4.13$$

$$Q_f = -B_{ss}V_s^{\ 2} + (G_{sr}\sin\delta_{sr} - B_{sr}\cos\delta_{sr})V_sV_r \qquad 4.14$$

$$P_r = G_{rr}V_r^{\ 2} + (G_{rs}\cos\delta_{rs} + B_{rs}\sin\delta_{rs})V_sV_r \qquad 4.15$$

$$Q_r = -B_{rr}V_r^{\ 2} + (G_{rs}\sin\delta_{rs} - B_{rs}\cos\delta_{rs})V_sV_r \qquad 4.16$$

Where $\delta_{sr} = \delta_s - \delta_r = -\delta_{rs}$

Given the series impedance $Z = R + jX$ and above equations, the real and reactive power flow between two buses can therefore be calculated. And the apparent power constraints are due to thermal limits of transmission line are given as $S_{sr} \leq S_{max}$ and $S_{rs} \leq S_{max}$.

Like transmission lines, the transformer has been modelled by its equivalent circuit and characterized by winding impedances Z, the exciting branch admittance Y, two buses to which the windings are connected and maximum MVA rating. The equivalent π circuit of a load tap-changer transformer is composed of an ideal transformer with a tap ratio, tap and admittance.

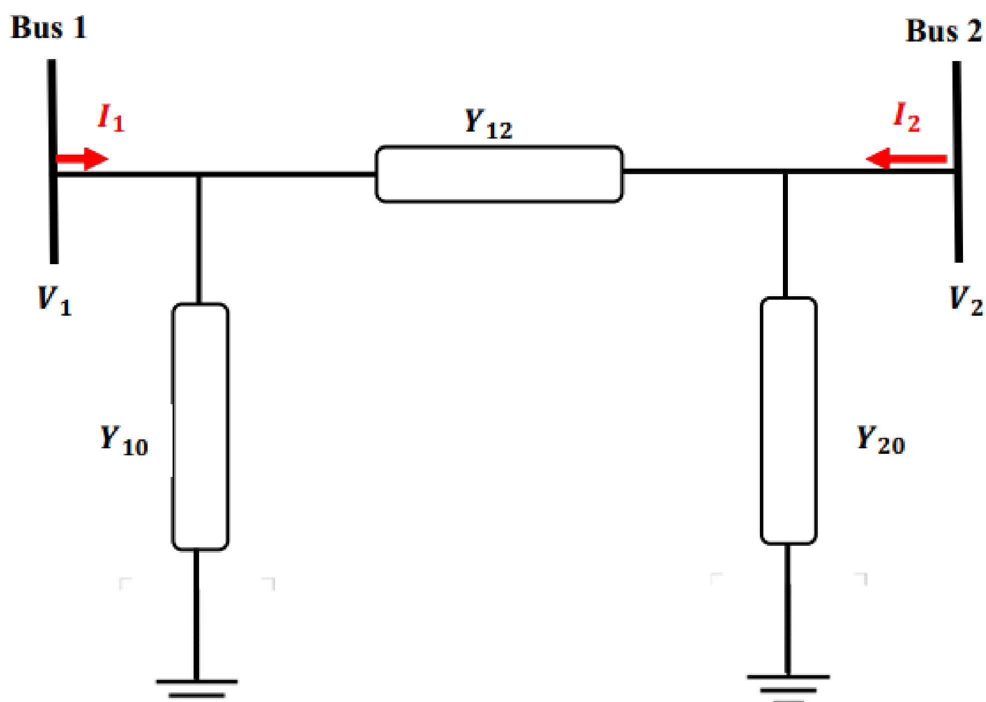

Figure 4.4: Equivalent π circuit of a transformer

The apparent powers S_1 and S_2 injected to the buses 1 and 2 respectively are given as:

$$S_1 = V_1 {I_1}^* = V_1(Y_{11}V_1 + Y_{12}V_2)^* \quad 4.17$$

$$S_2 = V_2 {I_2}^* = V_2(Y_{21}V_1 + Y_{22}V_2)^* \quad 4.18$$

Therefore, the injected real and reactive power flow 1 and 2 are found as:

$$P_1 = G'_{11}{V_1}^2 + (G'_{12}\cos\delta_{12} + B'_{12}\sin\delta_{12})V_1V_2 \quad 4.19$$

$$Q_1 = -B'_{11}{V_1}^2 + (G'_{12}\sin\delta_{12} - B'_{12}\cos\delta_{12})V_1V_2 \quad 4.20$$

$$P_2 = G'_{22}{V_2}^2 + (G'_{21}\cos\delta_{21} + B'_{21}\sin\delta_{21})V_1V_2 \quad 4.21$$

$$Q_2 = -B'_{22}{V_2}^2 + (G'_{21}\sin\delta_{21} - B'_{21}\cos\delta_{21})V_2V_1 \quad 4.22$$

Whereby,

$G'_{11} = \frac{R}{tap^2}$, $B'_{11} = \frac{X+j\frac{B_c}{2}}{tap^2}$, $G'_{22} = R$, $B'_{22} = X + j\frac{B_c}{2}$, $G'_{12} = G'_{21} = -\frac{R}{tap}$, $B'_{12} = B'_{21} = -\frac{X}{tap}$ and $\delta_{12} = \delta_1 - \delta_2 = -\delta_{21}$

As well, the elements of transformer model are found as:

$$Y_{10} = Y'_{11} - Y'_{12} = Y\left(\frac{1}{tap^2} - \frac{1}{tap}\right) + \frac{j\frac{B_c}{2}}{tap^2}$$

$$Y_{12} = Y'_{12} = -\frac{Y}{tap}$$

$$Y_{20} = Y'_{22} - Y'_{f12} = Y\left(1 - \frac{1}{tap}\right) + j\frac{B_c}{2}$$

The apparent powers are obtained from real and reactive power flow from bus 1 to bus 2 (P_{12} and Q_{12}) and from bus 2 to bus 1 (P_{21} and Q_{21}) of a line having series impedance $Z = R + jX$ and a load-tap-changer (LTC):

$$S_{12} = P_{12} + jQ_{12} = V_1 I_{12}^* \quad 4.23$$

$$S_{21} = P_{21} + jQ_{21} = V_2 I_{21}^* \quad 4.24$$

Where $P_{12} + jQ_{12} = P_1 + jQ_1$ and $P_{21} + jQ_{21} = P_2 + jQ_2$

Generally, the admittance matrix Y_{bus} can be obtained from line and transformer input data, whereby, diagonal elements, Y_i=sum of admittances connected to bus i and off-diagonal elements, Y_{ij}= - (sum of admittances connected between buses i and j), $i \neq j$.

In fact, the power flow equation can be written as [13]:

$$\sum_j Y_{ij}V_{ij} + Y_i^{sh}V_i = \frac{S_i^*}{V_i^*} \tag{4.25}$$

Where Y_{ij} is admittance matrix, Y_i^{sh} is the bus shunt admittance, V_i is the specified voltage at bus i and S_i is the bus power injection which represents a constant power loads and generators.

$$I_i = V_i \sum_{j=0}^{n} y_{ij} - \sum_{j=1}^{n} y_{ij}V_j, \qquad j \neq i \tag{4.26}$$

The real and reactive power at bus i can be found from the equations.

$$P_i + jQ_i = V_i I_i^* \tag{4.27}$$

$$I_i = \frac{P_i - jQ_i}{V_i^*} \tag{4.28}$$

Thus,

$$\frac{P_i - jQ_i}{V_i^*} = V_i \sum_{j=0}^{n} y_{ij} - \sum_{j=1}^{n} y_{ij}V_j, \qquad j \neq i \tag{4.29}$$

By separating the real and imaginary parts:

$$P_i = \sum_{j=1}^{n} |V_i| \left|V_j\right| \left|V_{ij}\right| \cos\left(\delta_{ij} - \delta_i + \delta_j\right) \tag{4.30}$$

$$Q_i = -\sum_{j=1}^{n} |V_i| \left|V_j\right| \left|V_{ij}\right| \sin(\delta_{ij} - \delta_i + \delta_j) \tag{4.31}$$

4.2.3. GENERATION AND LOAD MODELS

Since the generator is operated in steady state to deliver a given power at a fixed voltage V_G due to a voltage regulator. Therefore, the generation system element has been modeled as constant real power P_G and constant voltage magnitude V_G at PV bus according to the figure 4.5.

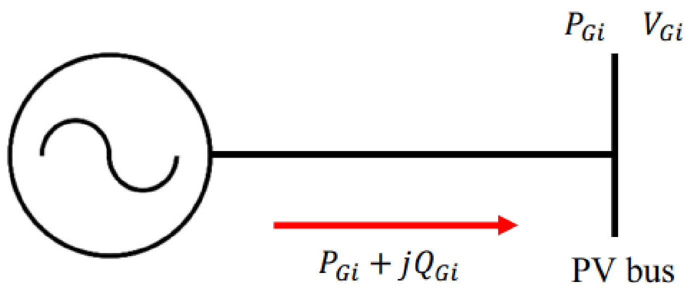

Figure 4.5: Equivalent circuit of an electrical generating systems

Therefore, generation unit is modeled as an active and reactive power injection as P_{Gi} and Q_{Gi} to the generation busbar respectively.

In this case, P_{Gi} and Q_{Gi} have to be maintained within certain limits to represent the mechanical system and electric current constraints such as $P_{Gi}^{min} \leq P_{Gi} \leq P_{Gi}^{max}$ and $Q_{Gi}^{min} \leq Q_{Gi} \leq Q_{Gi}^{max}$.

On the other hand, the loads have generally been modelled as constant impedances "Z" in the consideration that they are in steady state.

4.2.4. STATCOM MODEL

The STATCOM is normally modeled according to the parameter that it is intended to control. It has the capabilities to control the bus voltage, reactive power, impedance and current. Let a STATCOM be connected in shunt on bus i of a transmission line as shown on the figure 4.6.

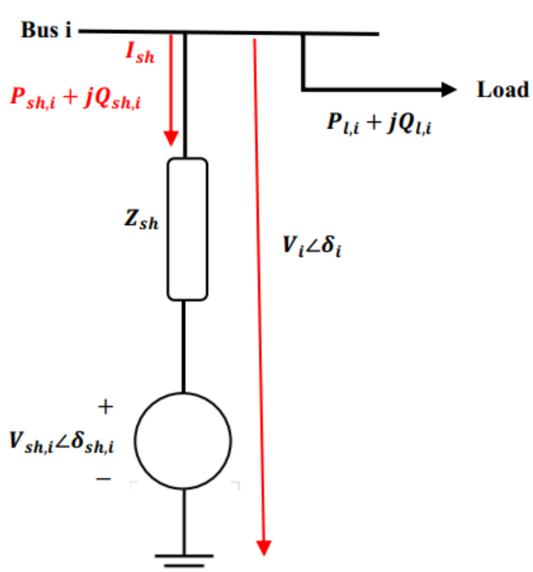

Figure 4.6: STATCOM equivalent circuit[6]

$$P_{sh,i} = V_i^2 G_{sh} - V_i V_{sh}(G_{sh}\,\mathrm{COS}(\delta_i - \delta_{sh}) + B_{sh}\,\mathrm{SIN}(\delta_i - \delta_{sh})) \quad 4.32$$

$$Q_{sh,i} = -V_i^2 B_{sh} - V_i V_{sh}(G_{sh}\,\mathrm{SIN}(\delta_i - \delta_{sh}) - B_{sh}\,\mathrm{COS}(\delta_i - \delta_{sh})) \quad 4.33$$

Whereby, $G_{sh} + B_{sh} = \frac{1}{Z_{sh}}$

The general equation of a multifunctional STATCOM is

$$\Delta F(x) = F(x, f^{ref}) = 0 \quad 4.34$$

Where $x = [\delta_1, V_1, \dots \delta_N, V_N, \delta_{sh}, V_{sh}\,]^t$, f^{ref} is a control reference.

Since there is no active power exchange through a DC link, the operating constraint of a STATCOM becomes:

$$PE = Re(V_{sh} I_{sh}^*) = V_i^2 G_{sh} - V_i V_{sh}(G_{sh}\,\mathrm{COS}(\delta_i - \delta_{sh}) + B_{sh}\,\mathrm{SIN}(\delta_i - \delta_{sh})) = 0 \quad 4.35$$

The additional constraints are:

- For the bus voltage control

$$V_i - V_i^{ref} = 0 \quad 4.36$$

Where V_i^{ref} is the reference bus voltage.

- Internal voltage and thermal constraints

$$V_{sh}^{min} \le V_{sh} \le V_{sh}^{max} \quad 4.37$$

$$-\pi \le \delta_{sh} \le \pi \quad 4.38$$

$$I_{sh} \le I_{sh}^{max} \quad 4.39$$

Where V_{sh}^{min}, V_{sh}^{max} and I_{sh}^{max} are minimum and maximum voltages and current ratings of STATCOM respectively.

$$I_{sh} = \left|\frac{(V_i - V_{sh})}{Z_{sh}}\right| \quad 4.40$$

- External voltage constraints

$$V_i^{min} \le V_i \le V_i^{max} \quad 4.41$$

$V_j^{min} \leq V_j \leq V_j^{max}$ 4.42

Where V_i^{min} and V_i^{max} are minimum and maximum voltages at local bus i and V_j^{min} and V_i^{max} stand for the minimum and maximum voltages at remote bus j.

Since the study is intended to control the bus voltage by means of controlling the reactive power, the Newton Raphson power flow for Kigali HV network has thus become:

$$\begin{bmatrix} \frac{\partial PE}{\partial \delta_{sh}} & \frac{\partial PE}{\partial V_{sh}} & \frac{\partial PE}{\partial \delta_1} & \frac{\partial PE}{\partial V_1} & \cdots & 0 & 0 \\ \frac{\partial P_1}{\partial \delta_{sh}} & \frac{\partial P_1}{\partial V_{sh}} & \frac{\partial P_1}{\partial \delta_1} & \frac{\partial P_1}{\partial V_1} & \cdots & \frac{\partial P_1}{\partial \delta_N} & \frac{\partial P_1}{\partial V_N} \\ \frac{\partial Q_1}{\partial \delta_{sh}} & \frac{\partial Q_1}{\partial V_{sh}} & \frac{\partial Q_1}{\partial \delta_1} & \frac{\partial Q_1}{\partial V_1} & \cdots & \frac{\partial Q_1}{\partial \delta_N} & \frac{\partial Q_1}{\partial V_N} \\ \vdots & \vdots & \vdots & \vdots & \ddots & \vdots & \vdots \\ 0 & 0 & \frac{\partial P_N}{\partial \delta_1} & \frac{\partial P_N}{\partial V_1} & \cdots & \frac{\partial P_N}{\partial \delta_N} & \frac{\partial P_N}{\partial V_N} \\ 0 & 0 & \frac{\partial Q_N}{\partial \delta_1} & \frac{\partial Q_N}{\partial V_1} & \cdots & \frac{\partial Q_N}{\partial \delta_N} & \frac{\partial Q_N}{\partial V_N} \end{bmatrix}_{N=12} \begin{bmatrix} \Delta\delta_{sh} \\ \Delta V_{sh} \\ \Delta\delta_1 \\ \Delta V_1 \\ \vdots \\ \Delta\delta_N \\ \Delta V_N \end{bmatrix} = \begin{bmatrix} -\Delta PE \\ -\Delta P_1 \\ -\Delta Q_1 \\ \vdots \\ \Delta P_N \\ \Delta Q_N \end{bmatrix}_{N=12} \quad 4.43$$

The STATCOM has two state variables δ_{sh} and V_{sh} and considers the active power balance from the equation 4.34 while the internal control constraint from the equation 4.34.

4.2.5. SSSC MODEL

SSSC has capabilities to control the active and reactive power flow, bus voltage and impedance of transmission line. It has characterized by its regulated voltage source V_{se} in series with a transformer impedance Z_{se}. The equivalent circuit of SSSC is shown in the figure 4.7.

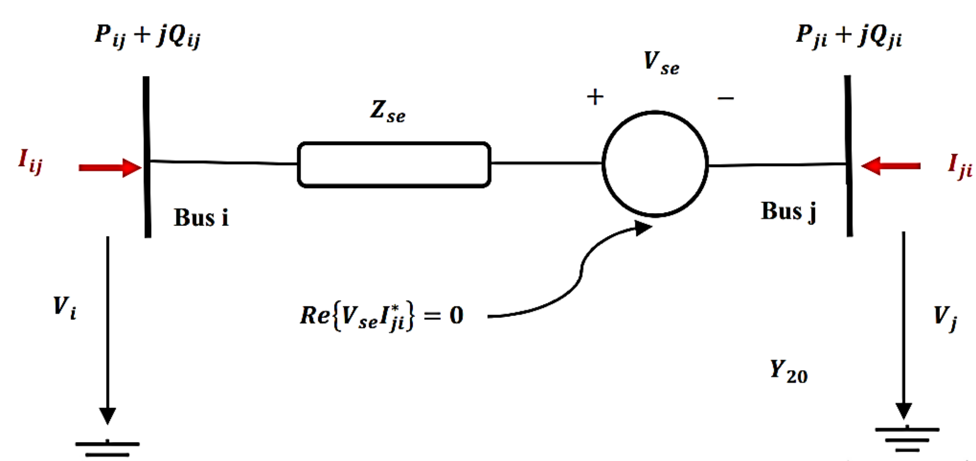

Figure 4.7: Equivalent circuit of SSSC [6]

The power flow constraints become:

$$P_{ij} = V_i^2 G_{ii} - V_i V_j \left(G_{ij} cos\delta_{ij} + B_{ij} sin\delta_{ij}\right) - V_i V_{se}[G_{ij} \cos(\delta_i - \delta_{se}) + B_{ij} \sin(\delta_i - \delta_{se})] \quad 4.44$$

$$Q_{ij} = -V_i^2 B_{ii} - V_i V_j \left(G_{ij} sin\delta_{ij} + B_{ij} cos\delta_{ij}\right) - V_i V_{se}[G_{ij} \sin(\delta_i - \delta_{se}) + B_{ij} \cos(\delta_i - \delta_{se})] \quad 4.45$$

$$P_{ji} = V_j^2 G_{jj} - V_j V_i \left(G_{ji} cos\delta_{ji} + B_{ji} sin\delta_{ji}\right) - V_j V_{se}[G_{ji} \cos\left(\delta_j - \delta_{se}\right) + B_{ji} \sin\left(\delta_j - \delta_{se}\right)] \quad 4.46$$

$$Q_{ji} = -V_j^2 B_{jj} - V_j V_i \left(G_{ji} sin\delta_{ji} + B_{ji} cos\delta_{ji}\right) - V_j V_{se}[G_{ji} \sin\left(\delta_j - \delta_{se}\right) + B_{ji} \cos\left(\delta_j - \delta_{se}\right)] \quad 4.47$$

Where $V_{se} = V_{se} \angle \delta_{se}$, $V_i = V_i \angle \delta_i$ and $V_j = V_j \angle \delta_j$, $G_{ij} + jB_{ij} = \frac{1}{Z_{se}}$, $G_{ii} = G_{jj} = G_{ij}$ and $B_{ii} = B_{jj} = B_{ij}$

The operating constraint is that there is no active power exchange via the DC link as per equation 4.48.

$$PE = Re\left(V_{se} I_{ji}^*\right) = -V_i V_{se}\left[G_{ij} \cos(\delta_i - \delta_{se}) + B_{ij} \sin(\delta_i - \delta_{se})\right] + V_j V_{se}[G_{ji} \cos\left(\delta_j - \delta_{se}\right) + B_{ji} \sin\left(\delta_j - \delta_{se}\right)] = 0 \quad 4.48$$

In order to control the bus voltage, the equation 4.49 becomes a constraint.

$$V_i - V_i^{ref} = 0 \text{ and } V_j - V_j^{ref} = 0 \quad 4.49$$

Where V_i^{ref} and V_j^{ref} are the reference bus voltages.

The SSSC is also constrained by internal voltage and current.

$$0 \leq V_{se} \leq V_{se}^{max} \quad 4.50$$

$$I_{se} \leq I_{se}^{max} \quad 4.51$$

$$-\pi \leq \delta_{se} \leq \pi \quad 4.52$$

V_{se}^{max} and I_{se}^{max} are SSSC current and voltage ratings.

$$I_{se} = I_{se} \angle \delta_{se} = \frac{V_i - V_{se} - V_j}{Z_{se}} \quad 4.53$$

Since the study is intended to control the bus voltage by means of controlling the reactive power, the Newton Raphson power flow for Kigali HV network has thus become:

$$
\begin{bmatrix}
\frac{\partial PE}{\partial \delta_{se}} & \frac{\partial PE}{\partial V_{se}} & \frac{\partial PE}{\partial \delta_i} & \frac{\partial PE}{\partial V_i} & \frac{\partial PE}{\partial \delta_j} & \frac{\partial PE}{\partial V_j} \\
\frac{\partial P_i}{\partial \delta_{se}} & \frac{\partial P_i}{\partial V_{se}} & \frac{\partial P_i}{\partial \delta_i} & \frac{\partial P_i}{\partial V_i} & \frac{\partial P_i}{\partial \delta_j} & \frac{\partial P_i}{\partial V_j} \\
\frac{\partial Q_i}{\partial \delta_{se}} & \frac{\partial Q_i}{\partial V_{se}} & \frac{\partial Q_i}{\partial \delta_i} & \frac{\partial Q_i}{\partial V_i} & \frac{\partial Q_i}{\partial \delta_j} & \frac{\partial Q_i}{\partial V_j} \\
\frac{\partial P_j}{\partial \delta_{se}} & \frac{\partial P_j}{\partial V_{se}} & \frac{\partial P_j}{\partial \delta_i} & \frac{\partial P_j}{\partial V_i} & \frac{\partial P_j}{\partial \delta_j} & \frac{\partial P_j}{\partial V_j} \\
\frac{\partial Q_j}{\partial \delta_{se}} & \frac{\partial Q_j}{\partial V_{se}} & \frac{\partial Q_j}{\partial \delta_i} & \frac{\partial Q_j}{\partial V_i} & \frac{\partial Q_j}{\partial \delta_j} & \frac{\partial Q_j}{\partial V_j}
\end{bmatrix}
\begin{bmatrix}
\Delta\delta_{se} \\ \Delta V_{se} \\ \Delta\delta_i \\ \Delta V_i \\ \Delta\delta_j \\ \Delta V_j
\end{bmatrix}_{i\neq j}
=
\begin{bmatrix}
-\Delta PE \\ -\Delta P_i \\ -\Delta Q_i \\ \Delta P_j \\ \Delta Q_j
\end{bmatrix}_{i\neq j}
\qquad 4.54
$$

On the other hand, it was studied that each of Shango, Rubavu, Kibuye and Juru substations could cause a complete blackout anytime its protection systems malfunction [24]. In this study, it has been observed that Shango, Gahanga na Rilima 110 kV buses have abnormal voltages. Therefore, it was recommended to install STATCOM at 110kV Shango bus and SSSC is proposed between Gahanga and Rilima 110kV buses in order to keep the voltage at each bus in Kigali HV network within the acceptable range.

4.3. SIMULATION OF KIGALI HIGH VOLTAGE NETWORK

Kigali HV network has been simulated with and without STATCOM and SSSC under normal and abnormal condition in order to ensure its level of stability. The model of the existing HV network is characterized by all existing power generation and current peak load which are connected to the respective bus as shown in the figure 4.8. The model of the future network is composed of the existing and planned generation capacity excluding the oil-based thermal generation from Birembo, Masoro, Jabana and Mukungwa power plants. This model also considers the forecasted peak load at each bus in Kigali zone as displayed in the figure 4.9.

The figure 4.10 provides the simulation architecture and voltage profile for future Kigali HV network with STATCOM and SSSC under steady state condition, whereas the model and results for future network with STATCOM and SSSC under normal and faulty conditions have been displayed in the figures from 4.11 to 4.15.

On the other hand, each model has the system solver, scopes, displays, voltage and current measurement elements; conversion as well as control systems in order to let the circuit be functional and facilitate on the results displaying.

4.3.1. SIMULATION OF KIGALI NETWORK WITHOUT FACTS DEVICES

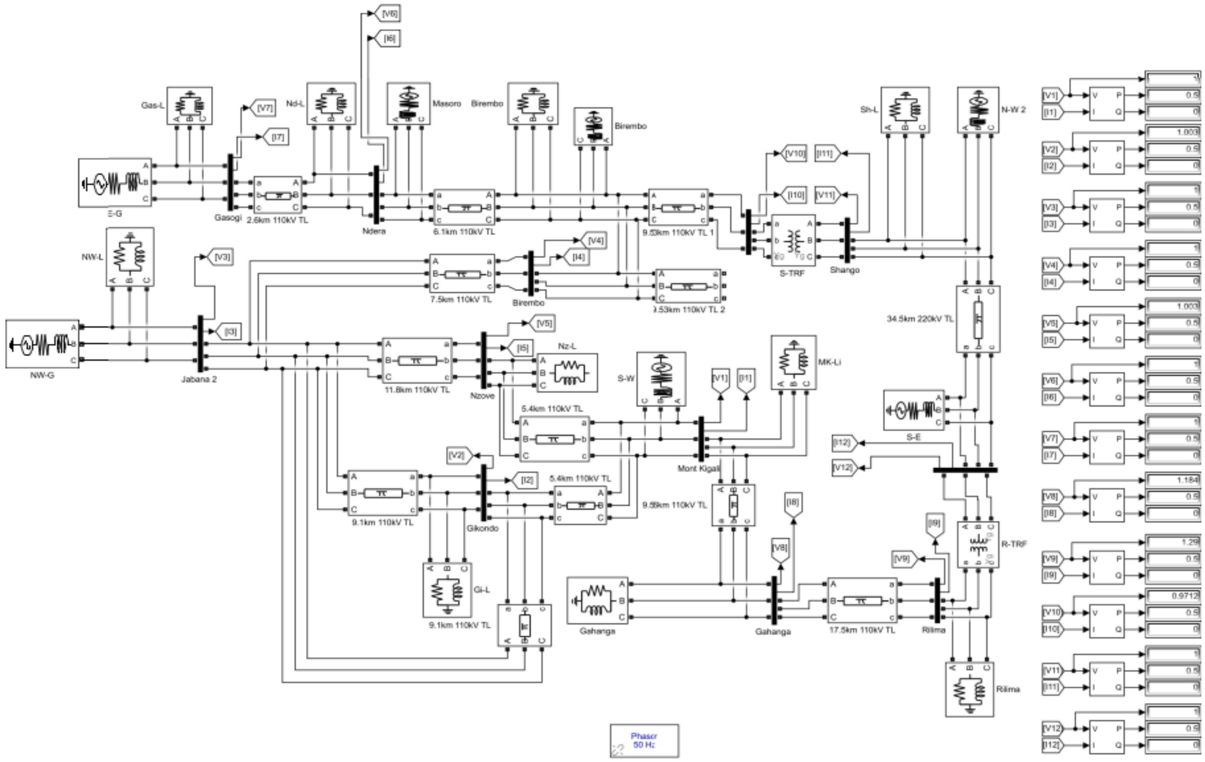

Figure 4.8: Simulation model of the existing HV network 2023 without FACTS devices

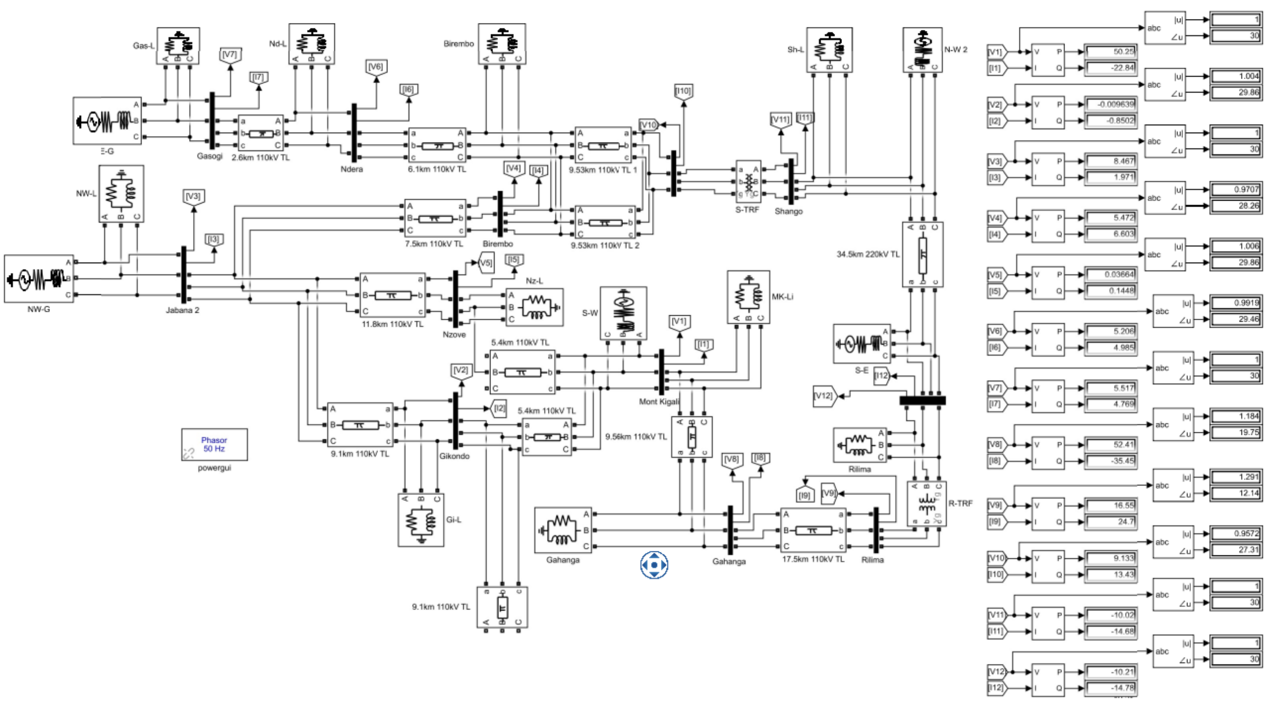

Figure 4.9: Simulation model of future HV network without FACTS devices

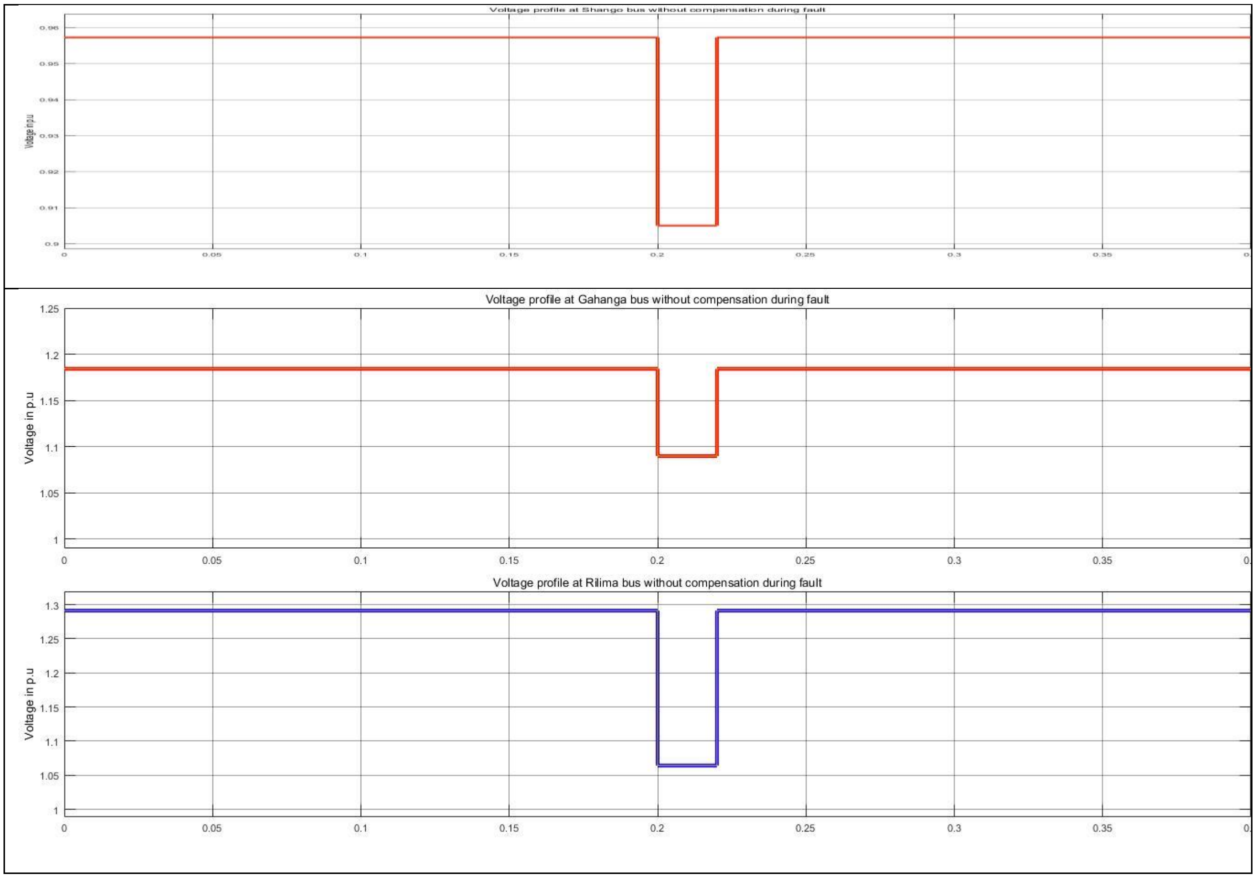

Figure 4.10: Critical bus voltage profile under fault condition

4.3.2. SIMULATION OF KIGALI HV NETWORK WITH STATCOM AND SSSC

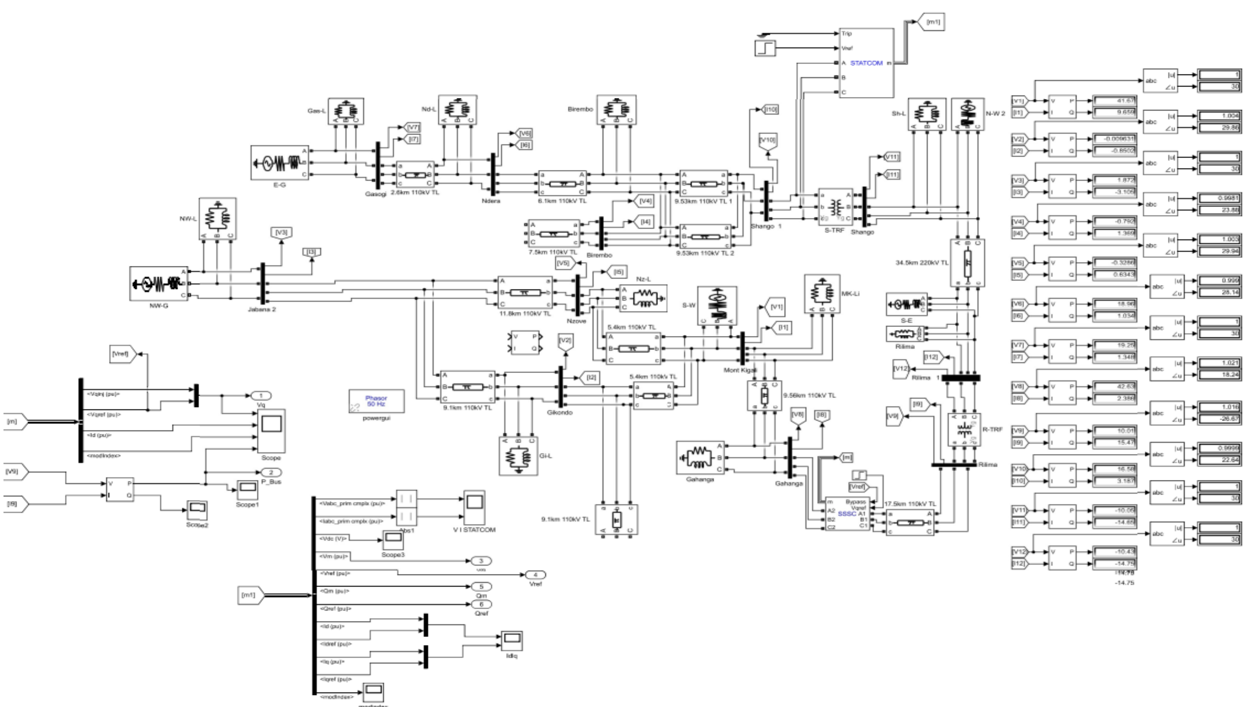

Figure 4.11: Simulation model of HV network with STATCOM and SSSC

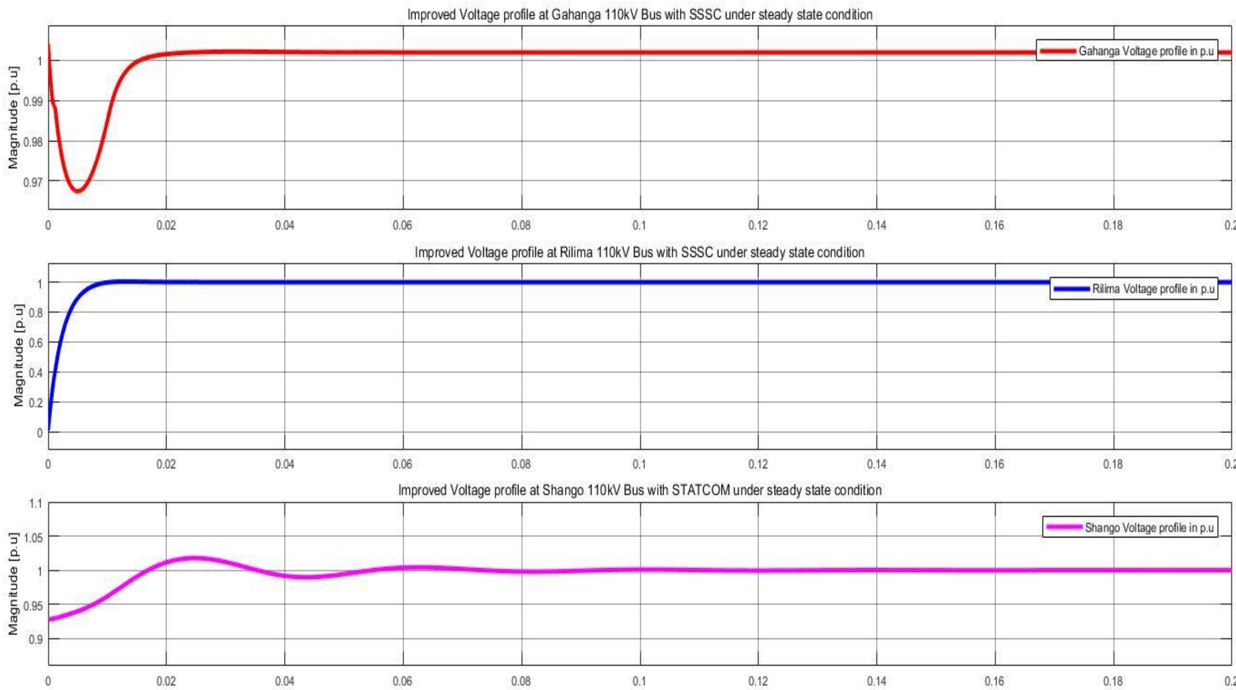

Figure 4.12: Improved Voltage profile at three critical 110kV buses

4.3.3. SIMULATION OF KIGALI HV NETWORK WITH STATCOM

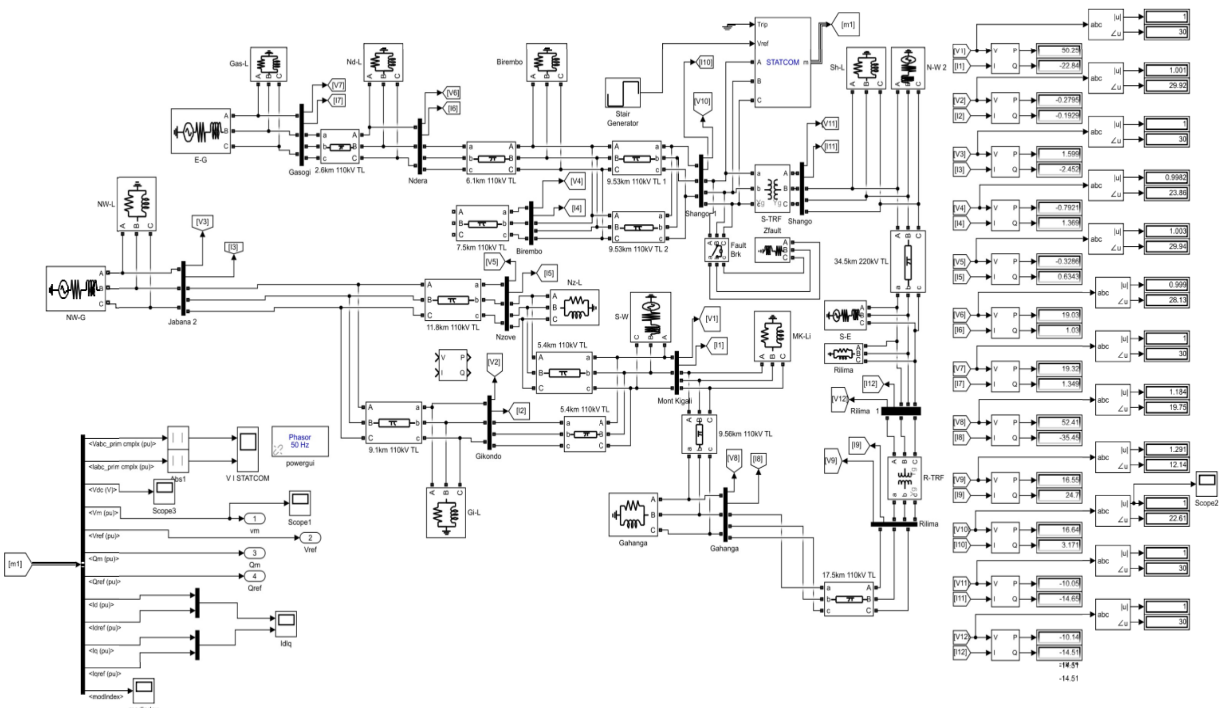

Figure 4.13: Simulation model of HV network with STATCOM

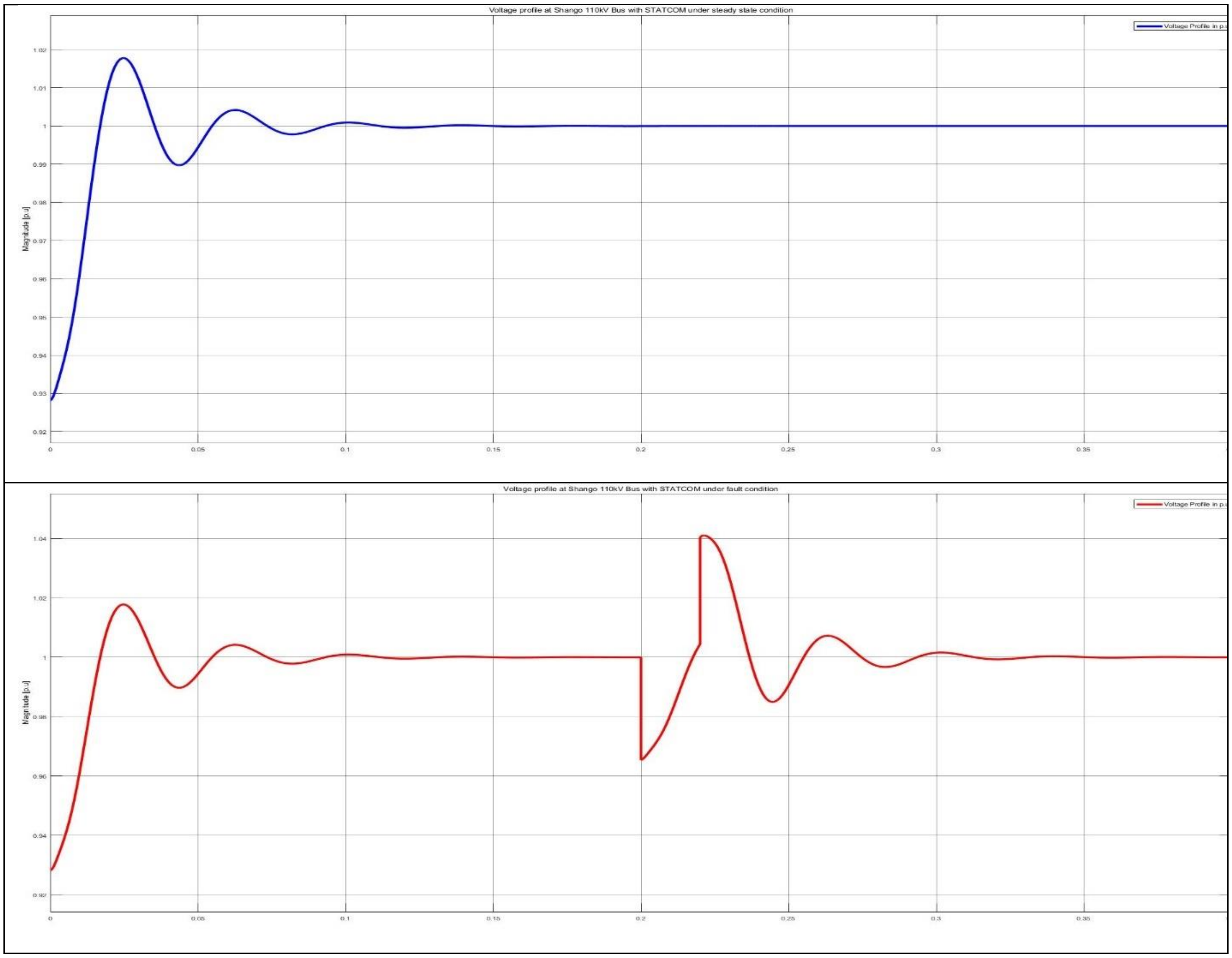

Figure 4.14: Voltage profile at Shango 110kV bus under steady state and fault condition

4.3.4. SIMULATION OF KIGALI HV NETWORK WITH SSSC

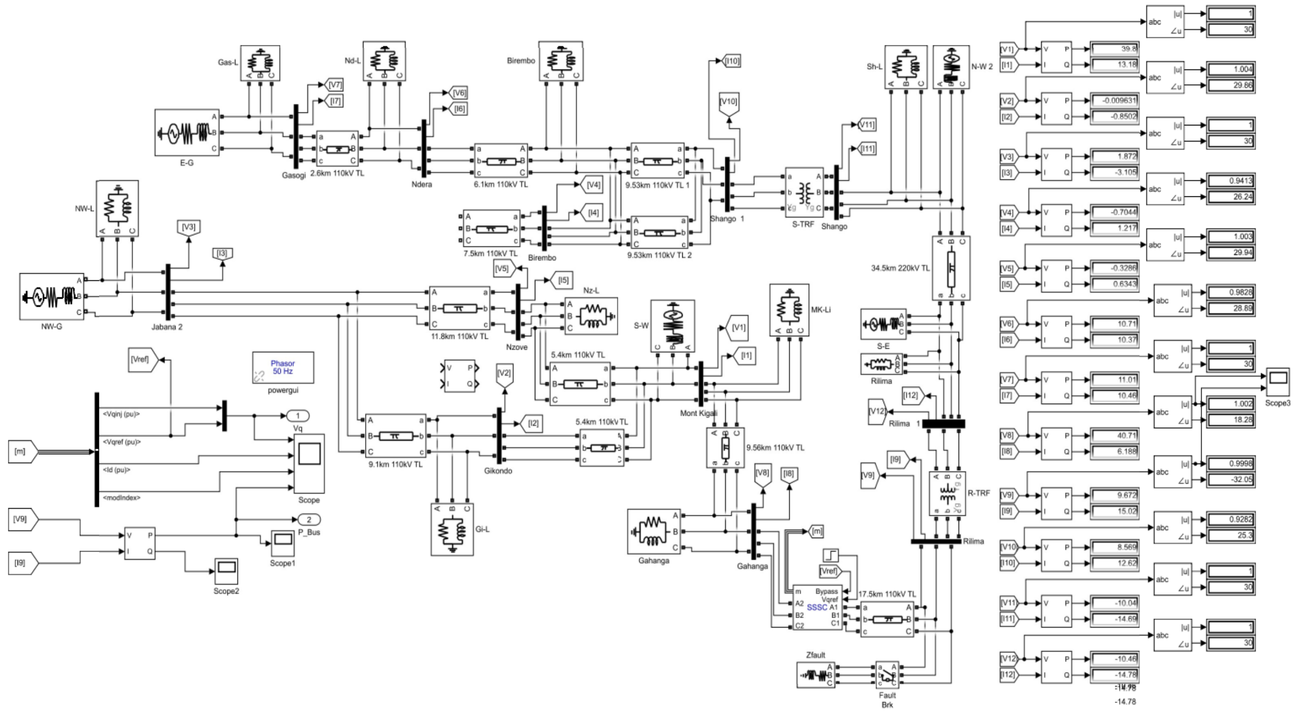

Figure 4.15: Simulation model of HV network with SSSC

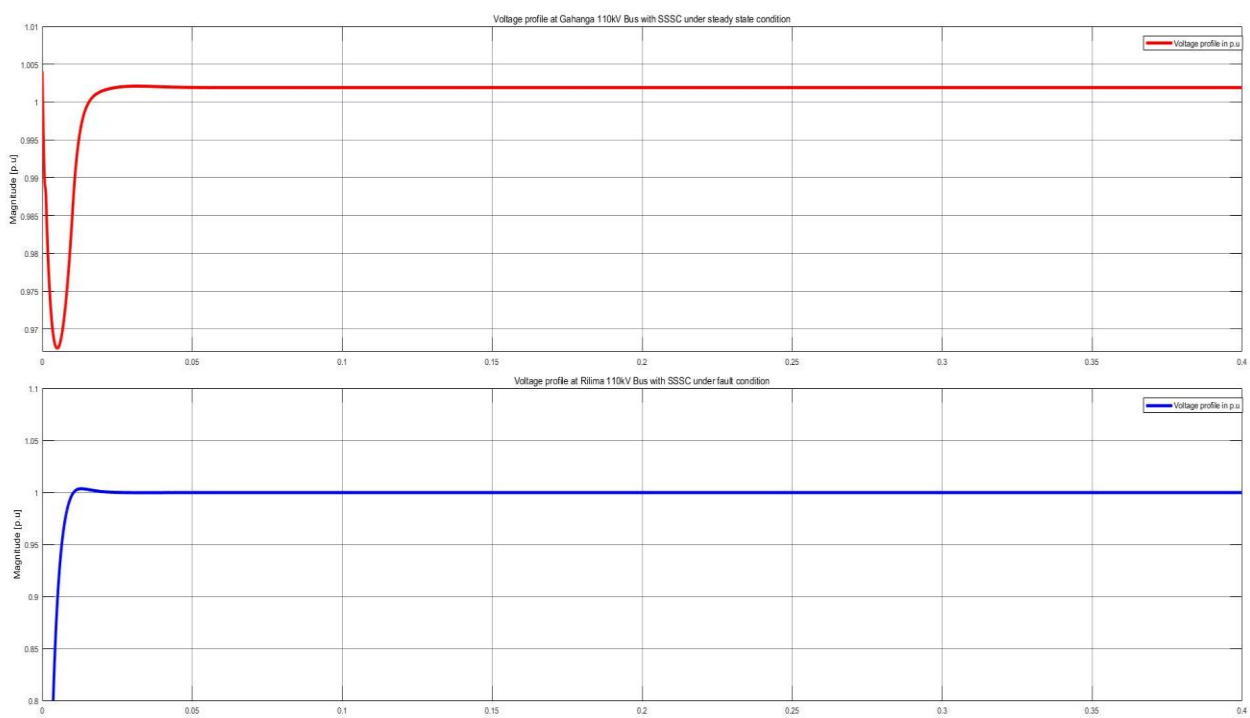

Figure 4.16: Voltage profile at Gahanga and Rilima 110kV buses under steady state condition

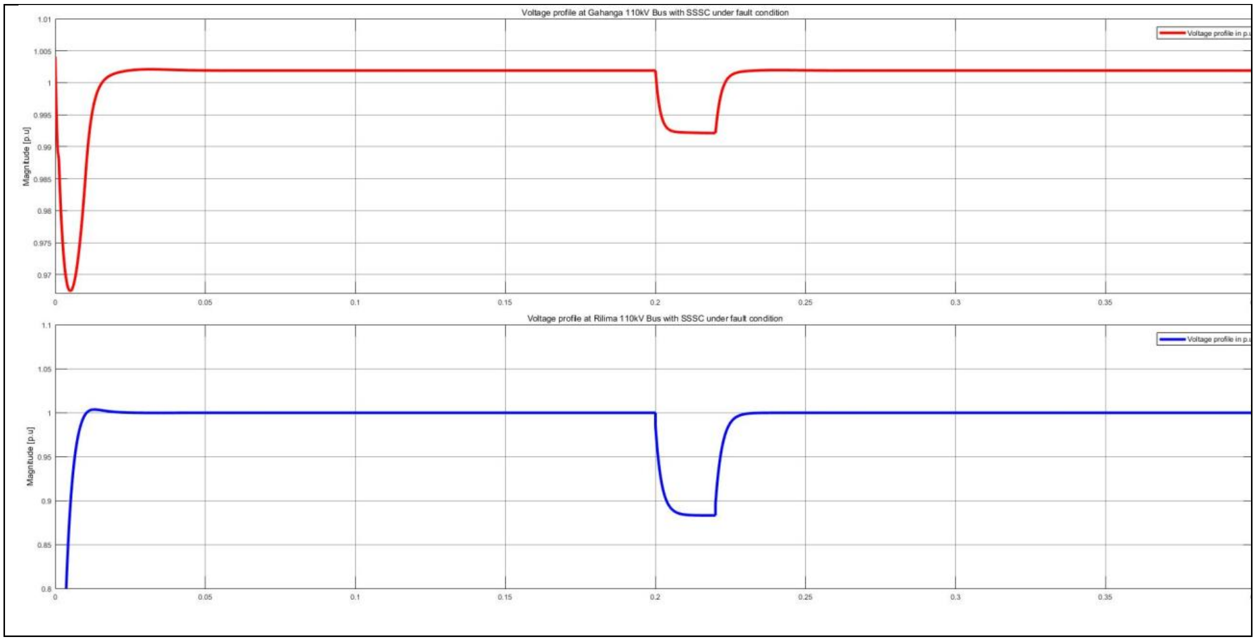

Figure 4.17: Voltage profile at Gahanga and Rilima 110kV buses under fault condition

4.3.5. RESULTS INTERPRETATION

This section described the obtained results from different performed simulations of Kigali HV network in the previous section. In fact, the existing and future HV network have modelled and simulated in the Matlab/Simulink environment and the results are compared with the applicable standard requirements as per table 4.1.

Table 4.1: Recorded simulation results

Buses	Steady State Voltage in p.u					
	Standard [25]	Kigali 2023 without FACTS	Kigali 2032 without FACTS	Kigali 2032 with STATCOM	Kigali 2032 with SSSC	Kigali 2032 with STATCOM and SSSC
1. Mont Kigali	0.95~1.05	1	1	1	1	1
2. Gikondo	0.95~1.05	1.003	1.004	1.001	1.001	1.004
3. Jabana 2	0.95~1.05	1	1	1	1	1
4. Birembo	0.95~1.05	1	0.9707	0.9982	**0.9413**	0.9982
5. Nzove	0.95~1.05	1.003	1.006	1.003	1.003	1.003
6. Ndera	0.95~1.05	1	0.9919	0.999	0.9828	0.999
7. Gasogi	0.95~1.05	1	1	1	1	1
8. Gahanga	0.95~1.05	**1.185**	**1.184**	**1.184**	1.002	1.002
9. Rilima	0.95~1.05	**1.292**	**1.291**	**1.291**	0.9998	0.9998
10. Shango	0.95~1.05	0.9861	**0.9572**	1	**0.9282**	1
11. Shango	0.95~1.05	1	1	1	1	1
12. Rilima	0.95~1.05	1	1	1	1	1

According to the table 4.2, the voltage profiles for all buses in Kigali HV network has been improved within acceptable with the integrated STATCOM and SSSC. The use of only one FACTS device is not enough to improve the voltage profile.

During the disturbances, the simulation results have confirmed that the SSSC and STATCOM can maintain the system voltage within the acceptable range as per figure 3.2. In this study, a fault of 0.02 seconds has been applied to the critical buses and the results have been compared. Table 4.2 shows that the SSSC can contribute for damping the transient voltage amplitude, whereas, the STATCOM has however increased the transient voltage amplitude as well as fault settling time.

Table 4.2: Network disturbances assessment

Critical bus	Without FACTS		With FACTS at critical buses	
	Voltage variation during fault in %	Fault settling time in second	Voltage variation during fault in %	Fault settling time in second
Shango	4.5%	0.02	7%	0.15
Gahanga	10%	0.02	0.9%	0.02
Rilima	23%	0.02	11%	0.02

CHAPTER 5. CONCLUSION AND RECOMMENDATIONS

5.1. CONCLUSION

During this study, it is observed that the system stability depends on the voltage profile across the system, whereas the voltage is affected by changes in reactive power flow. In view of these considerations, the FACTS devices have been described and employed to supply or consume reactive power whether they are producing active power or not, for the purpose of voltage control. Therefore, the results showed STATCOM and SSSC controllers have improved the voltage profile within the range between 0.9982 to 1.004 p.u. In addition, the SSSC has been found to be a contributing controller on both voltage improvement and damping the voltage transients as compared to the STATCOM. Since FACTS devices are electronically controlled, the design of efficient control system is also another key factor for the optimization of the FACTS performance.

Therefore, the use of STATCOM and SSSC is feasible to maintain the bus voltage within acceptable ranges and improve the stability of Kigali HV network.

5.2. RECOMMENDATIONS

The further research is recommended especially on the optimization and paybacks from power flow control, increase of transmission capability, reactive power compensation, stability improvement, power quality improvement, power conditioning, flicker mitigation, and interconnection of renewable and distributed generation and storages.

REFERENCES

[1] REG, “Annual report 2021-2022.pdf.” p. 31, 2022. [Online]. Available: https://www.reg.rw/fileadmin/user_upload/REG_Annual_report_2021-2022.pdf

[2] S. Mohammad and S. Am, “Transient stability improvement and osciallation damping by using SMES et de SSSC Seyed Mohammad Sadeghzadeh,” 2013.

[3] EUCL, “Annual Report 2021/2022,” 2022.

[4] MININFRA, “Rwanda Energy Policy,” 2015. [Online]. Available: https://www.reg.rw/fileadmin/user_upload/Rwanda_energy_policy-21612.pdf

[5] NISR, “Population projections,” Kigali, Rwanda, 2014. [Online]. Available: https://www.statistics.gov.rw/publication/rphc4-population-projections

[6] B. P. Xiao-Ping, Christian Rehtanz, Flexible AC Transmission Systems: Modelling and Control. Springer-Verlag Berlin Heidelberg, 2012.

[7] B. Valani, “Power Quality Improvement by SSSC and STATCOM Fact Devices using PI Controller,” vol. 02, no. 03, pp. 31–36, 2016.

[8] S. S. M. Pradeep H. Kathar, “Comparative Analysis of STATCOM And SSSC To Improve Voltage Stability And Loss Reduction,” International Journal of Scientific & Technology Research, vol. 8, no. 12, pp. 8–11, 2019.

[9] A. Ghorbani, B. Mozafari, S. Soleymani, and A. M. Ranjbar, “Impact of STATCOM and SSSC on synchronous generator LOE protection,” Turkish Journal of Electrical Engineering and Computer Sciences, vol. 24, no. 4, pp. 2575–2588, 2016, doi: 10.3906/elk-1403-13.

[10] A. Antony and G. K. Mathew, “A Comparative Study on Power Quality Improvement in a Hybrid System Using DVR and STATCOM versus Distributed Power Flow Controller (DPFC),” pp. 544–550, 2016.

[11] S. Paul, M. Datta, and C. Nandi, “Controlling SSSC by Full Order State Feedback Controller,” Int J Comput Appl, vol. 151, no. 9, pp. 33–39, 2016, doi: 10.5120/ijca2016911868.

[12] Ronita Pawn and Prof. R. B. Thakre, “Comparative Study of Power System Stability Enhancement of Various IEEE Bus System using SSSC,” International Journal of Engineering Research and, vol. V5, no. 02, pp. 359–363, 2016, doi: 10.17577/ijertv5is020437.

[13] G. A. Adepoju, M. A. Sanusi, and M. A. Tijani, "Application of SSSC to the 330kV Nigerian transmission network for voltage control," Nigerian Journal of Technology, vol. 36, no. 4, p. 1258, 2018, doi: 10.4314/njt. v36i4.36.

[14] R. Yadav, V. Yadav, and P. Yadav, "Improvement in Rotor Stability in 3 Machine 9 Bus System Using TCSC, SVC , SSSC," vol. 5, no. 03, pp. 1–5, 2017.

[15] D. P. Kadam and P. B. E. Kushare, "Mitigation of Harmonics by using STATCOM," vol. 1, no. 1, pp. 331–335, 2013.

[16] N. Johansson, L. Ängquist, H. P. Nee, and B. Berggren, "A dynamic power flow controller for power system stability improvement and loss reduction," 16th Power Systems Computation Conference, PSCC 2008, no. January 2008.

[17] N. M. Khoa, N. H. Hieu, and D. T. Viet, "A Study of SVC ' s Impact Simulation and Analysis for Distance Protection Relay on Transmission Lines," International Journal of Electrical and Computer Engineering (IJECE), vol. 7, 2017.

[18] M. Mahdi, "Optimal Power Flow with FACTS Devices," no. April, pp. 46–60, 2004.

[19] B. Tamimi, C. Cañizares, and C. Battistelli, "Hybrid Power Flow Controller Steady-State Modeling, Control, and Practical Application," IEEE Transactions on Power Systems, vol. 32, no. 2, pp. 1483–1492, 2017, doi: 10.1109/TPWRS.2016.2587770.

[20] REG, "Annual report 2019-2020.pdf," 2020.

[21] REG, "Annual Report 2020-2021," 2021. [Online]. Available: https://www.reg.rw/fileadmin/REG_ANNUAL_REPORT_2020-2021_V3.pdf

[22] EUCL, "Status of the losses in Rwandan Power Grid and Loss Reduction Investment Plan," 2016.

[23] REG, "Least Cost Power Development Plan: June 2021," no. June, pp. 2020–2040, 2020.

[24] B. R. Sandra Harel and Lior Cohen, Avigdor Itzhack, "National Power Master Plan for Rwanda Transmission System, Final Report for the Years 2020-2025-2030, Part 3," 2020.

[25] RURA, "Rwanda Grid Code," no. August, p. 314, 2013.

APPENDICES

APPENDIX 1: REQUEST FOR DATA

FW: Request for facilitation to get data for academic use
3 messages

Theoneste Higaniro <thiganiro@edcl.reg.rw> 5 October 2023 at 15:52
To: Joseph Ntwali <jntwali@edcl.reg.rw>
Cc: "coalanicy@gmail.com" <coalanicy@gmail.com>, Jean Paul Rutembesa <jprutembesa@edcl.reg.rw>

It's fine,

We can provide possible data to him.

Regards

From: Joseph Ntwali <jntwali@edcl.reg.rw>
Sent: Thursday, October 5, 2023 10:25 AM
To: Theoneste Higaniro <thiganiro@edcl.reg.rw>
Subject: FW: Request for facilitation to get data for academic use

Dear Director,

I hope this finds you well. Is it possible to facilitate him?

Joseph Ntwali <jntwali@edcl.reg.rw> 5 October 2023 at 16:01
To: "ICYUZUZO A.Colombe" <coalanicy@gmail.com>, INFO EDCL <info@edcl.reg.rw>
Cc: BIKORIMANA JMV <jbikorimana27@gmail.com>

Dear Colombe,

Thank you for your mail below. Kindly liaise with the Director of Generation and Transmission for facilitation.

From: ICYUZUZO A.Colombe <coalanicy@gmail.com>
Sent: Wednesday, October 4, 2023 7:45 PM
To: INFO EDCL <info@edcl.reg.rw>

Cc: BIKORIMANA JMV <jbikorimana27@gmail.com>
Subject: Request for facilitation to get data for academic use

You don't often get email from coalanicy@gmail.com. Learn why this is important

Dear All,

Hope you are doing well!

This email serves to request for facilitation to get data for academic use.

I am looking forward to hearing from you.

--

Thank you and Best Regards,

APPENDIX 2: CURRENT AND FUTURE GENERATION STATUS

CURRENT SITUATION			FUTURE SITUATION		
Plant Name	**Type of plant**	**Capacity in MW**	**Plant Name**	**Type of plant**	**Capacity in MW**
Kigali Zone					
Jabana 1	Thermal Power	0.25	Kivuwatt 1	Methane Gas to Power	26.19
Jabana 2	Thermal Power	3.2	Kivuwatt 2	Methane Gas to Power	8
Masoro	Thermal Power	10	UETCL	Imported Power	2
Birembo	Thermal Power	10	SPLK	Methane Gas to Power	50
Kivuwatt 1	Methane Gas to Power	26.19	Rusumo Falls	Imported Hydropower	26.7
UETCL	Imported Power	2	-	-	-
SPLK	Methane Gas to Power	50	-	-	-
	Total	**101.64**		**Total**	**112.89**
South-Western Zone					
Nshili	Hydropower	0.4	Nshili	Hydropower	0.4
Nyabarongo 1	Hydropower	28	Nyabarongo 1	Hydropower	28
Rukarara 1	Hydropower	9	Rukarara 1	Hydropower	9
Rukarara 2	Hydropower	2.2	Rukarara 2	Hydropower	2.2
Nyirantaruko	Hydropower	1.84	Nyirantaruko	Hydropower	1.84
Rukarara 5	Hydropower	5	Rukarara 5	Hydropower	5
Nkora	Hydropower	0.68	Nkora	Hydropower	0.68
Nyamyotsi 1	Hydropower	0.1	Nyamyotsi 1	Hydropower	0.1
Nyamyotsi 2	Hydropower	0.1	Nyamyotsi 2	Hydropower	0.1
Gishoma	Peat to Power	15	Gishoma	Peat-to-Power	15
Rusizi 1	Hydropower	4.1	Rusizi 1	Hydropower	4.1
Rusizi 2	Hydropower	12	Rusizi 2	Hydropower	12
-	-	-	Nyabarongo 2	Hydropower	37
-	-	-	Rukarara 6	Hydropower	6.7
-	-	-	Rusizi 3	Hydropower	48.3
	Total	**78.42**		**Total**	**170.42**
North-Western Zone					
Cyimbili	Hydropower	0.3	Cyimbili	Hydropower	0.3
Gashashi	Hydropower	0.28	Gashashi	Hydropower	0.28
Giciye 1	Hydropower	4	Giciye 1	Hydropower	4
Giciye 2	Hydropower	4	Giciye 2	Hydropower	4
Gihira	Hydropower	1.8	Gihira	Hydropower	1.8
Gisenyi	Hydropower	1.7	Gisenyi	Hydropower	1.7
Keya	Hydropower	2.2	Keya	Hydropower	2.2
Mazimeru	Hydropower	0.5	Mazimeru	Hydropower	0.5
Mukungwa 1	Hydropower	12	Mukungwa 1	Hydropower	12
Mukungwa 2	Hydropower	3.6	Mukungwa 2	Hydropower	3.6
Murunda	Hydropower	0.1	Murunda	Hydropower	0.1
Musarara	Hydropower	0.4	Musarara	Hydropower	0.4
Mutobo	Hydropower	0.2	Mutobo	Hydropower	0.2
Nkora	Hydropower	0.68	Nkora	Hydropower	0.68
Ntaruka	Hydropower	11.25	Ntaruka	Hydropower	11.25
Rugezi	Hydropower	2.6	Rugezi	Hydropower	2.6
Nyabahanga	Hydropower	0.2	Nyabahanga	Hydropower	0.2
Janja	Hydropower	0.2	Janja	Hydropower	0.2
Giciye 3	Hydropower	9.8	Giciye 3	Hydropower	9.8

Rubagabaga	Hydropower	0.45	Rubagabaga	Hydropower	0.45
Kigasa	Hydropower	0.272	Kigasa	Hydropower	0.272
Rwaza	Hydropower	2.6	Rwaza	Hydropower	2.6
Gaseke	Hydropower	0.5	Gaseke	Hydropower	0.5
Mukungwa	Thermal	10	KP1	Methane Gas to Power	3.6
KP1	Methane Gas to Power	3.6	Jali	Solar Power	0.25
Jali	Solar Power	0.25	Bihongore	Hydropower	5.35
	Total	**73.482**		**Total**	**68.832**
South-Eastern Zone					
Hakan	Peat to Power	35	Hakan 1	Peat to Power	35
-	-	-	Hakan 2	Peat to Power	40
	Total	35		Total	75
Eastern Zone					
Gigawatt Global	Solar to Power	8.5	Gigawatt Global	Solar to Power	8.5
Nasho	Solar to power	3.3	Nasho	Solar to power	3.3
	Total	**11.8**		**Total**	**11.8**

APPENDIX 3: HV TRANSMISSION LINES

From Bus name	To Bus name	Voltage Level [kV]	Rate [MVA]	R [p.u]	R [Ω]	X [p.u]	X [Ω]	B [p.u]	B [Ω]	Length [km]
Birembo	Jabana 2	110	108.6	0.01	1.60	0.03	3.02	0.00	0.25	7.5
Birembo	Ndera	110	108.6	0.01	1.30	0.02	2.45	0.00	0.21	6.1
Jabana 2	Gikondo	110	122.9	0.01	0.91	0.03	3.16	0.00	0.31	9.1
Gikondo	Mont Kigali	110	122.9	0.01	0.54	0.02	1.88	0.00	0.18	5.4
Ndera	Gasogi	110	108.6	0.00	0.55	0.01	1.05	0.00	0.09	2.6
Rilima (Bugesera)	Gahanga	110	122.7	0.01	0.86	0.05	4.72	0.01	0.72	17.5
Gahanga	Mont Kigali	110	122.9	0.01	0.96	0.03	3.32	0.00	0.32	9.56
Nzove	Jabana 1	110	122.9	0.01	1.18	0.04	4.10	0.00	0.40	11.8
Nzove	Mont Kigali	110	122.9	0.01	0.54	0.02	1.88	0.00	0.18	5.4
Birembo	Shango	110	245.8	0.01	0.51	0.03	1.68	0.00	0.15	9.53
Birembo	Shango	110	245.8	0.01	0.51	0.03	1.68	0.00	0.15	9.53
Rilima (Bugesera)	Shango	220	488	0.00	0.25	0.01	1.38	0.14	13.47	34.5

APPENDIX 4: HV TRANSFORMERS

Name	In service	Rating [MVA]	Voltage [kV]	Base rating [MVA]	Gm [p.u]	B_m [p.u]	Load Loss [p.u]	No-Load Loss [p.u]	No-Load Loss [p.u]	Vector Group
Rilima (Bugesera)	Yes	75/93.8	220/110/11	90	0.0006	0.0035 4	0.01	0.23	0.23	YNa0d1
Shango	Yes	75/93.8	220/110/11	90	0.0006	0.0035 4	0.01	0.23	0.23	YNa0d1
Kibuye	Not yet	75/93.8	220/110/11	90	0.0006	0.0035 4	0.01	0.23	0.23	YNa0d1
Rubavu	Not yet	75/93.8	220/110/11	90	0.0006	0.0035 4	0.01	0.23	0.23	YNa0d1

APPENDIX 5: CURRENT AND FORECASTED ELECTRICITY DEMAND PER SUBSTATION

S/S Name	Voltage Level [kV]	S/S Capacity [MVA]	2020			2021			2022			2023			2032		
			P	Q	S	P	Q	S	P	Q	S	P	Q	S	P	Q	S
Kigali Zone																	
Gikondo	110/15	45	27.1	27.9	38.9	29.2	30.1	41.9	32.1	33.1	46.1	35.3	36.4	50.7	83.3	85.8	119.6
Mont Kigali	110/15 &30	40	9.5	9.8	13.6	10.3	10.6	14.7	11.3	11.6	16.2	12.4	12.8	17.8	29.3	30.1	42.0
Jabana 1	110/15	20	12.9	13.3	18.5	13.9	14.3	20.0	15.3	15.7	21.9	16.8	17.3	24.1	39.7	40.8	56.9
Birembo	110/15	40	13.3	13.7	19.1	14.3	14.7	20.6	15.8	16.2	22.6	17.3	17.8	24.9	40.9	42.1	58.7
Gasogi	110/15	10	1.2	1.2	1.7	1.3	1.3	1.8	1.4	1.5	2.0	1.6	1.6	2.2	3.7	3.8	5.2
Ndera	110/15	40	7.0	7.2	10.1	7.6	7.8	10.9	8.4	8.6	12.0	9.2	9.5	13.2	21.7	22.3	31.1
Gahanga	110/15	20	6.8	7.0	9.7	7.3	7.5	10.5	8.0	8.3	11.5	8.8	9.1	12.7	20.9	21.5	29.9
Nzove	110/15	40	6.0	6.2	8.6	6.5	6.7	9.3	7.1	7.3	10.2	7.8	8.1	11.2	18.4	19.0	26.5
Rilima (Bugesera)	220/30	71.5	11.3	11.6	16.2	12.2	12.6	17.5	13.4	13.8	19.2	14.8	15.2	21.2	34.8	35.8	49.9
Shango (Shango, Rubavu - Kibuye)	220/30	126	11.3	11.6	11.9	12.1	12.5	12.9	13.3	13.7	14.1	14.7	15.1	15.6	34.6	35.6	49.7
Total			106.4	109.5	148.4	114.7	118.0	160.0	126.1	129.9	176.0	138.7	142.8	193.6	327.1	336.8	469.5
South-Western Zone																	
Kigoma	110/30	10	4.0	4.1	5.8	4.3	4.5	6.2	4.8	4.9	6.8	5.2	5.4	7.5	12.4	12.7	17.8
Kilinda	110/30	6	0.3	0.3	0.4	0.3	0.3	0.4	0.3	0.3	0.5	0.4	0.4	0.5	0.9	0.9	1.2
Karongi	110/30	10	4.5	4.7	6.5	4.9	5.0	7.0	5.4	5.5	7.7	5.9	6.1	8.5	14.0	14.4	20.0
Ntendezi	110/30	15	0.9	1.0	1.3	1.0	1.0	1.4	1.1	1.1	1.6	1.2	1.3	1.8	2.9	3.0	4.1
Rukarara	110/30	20	5.5	5.6	7.8	5.9	6.1	8.5	6.5	6.7	9.3	7.1	7.3	10.2	16.8	17.3	24.1
Bugarama	110/30	30	1.0	1.1	1.5	1.0	1.1	1.5	1.0	1.1	1.5	1.1	1.2	1.6	2.7	2.8	3.8
Mururu I	110/30	10	5.1	5.2	7.3	5.5	5.7	7.9	6.0	6.2	8.7	6.6	6.8	9.5	15.7	16.1	22.5

Kibogora	110/30	6	0.8	0.8	1.2	0.9	0.9	1.2	1.0	1.0	1.4	1.1	1.1	1.5	2.5	2.6	3.6
Gisagara	220/110/30	20	2.0	2.1	2.9	2.2	2.2	3.1	2.4	2.4	3.4	2.6	2.7	3.7	6.1	6.3	8.8
Huye (New)	110/30	20	-	-	-	-	-	-	-	-	-	-	-	-	4.9	5.0	7.0
Total			24.2	24.9	34.7	26.0	26.7	37.3	28.5	29.3	40.9	31.3	32.2	45.0	78.7	81.0	113.0
North-Western Zone																	
Mukungwa	110/30	15	8.4	8.7	12.1	9.1	9.3	13.0	10.0	10.3	14.3	11.0	11.3	15.8	25.9	26.7	37.2
Ntaruka	110/30	15	5.9	6.1	8.5	6.4	6.5	9.1	7.0	7.2	10.0	7.7	7.9	11.1	18.2	18.7	26.1
Rulindo	110/30	20	4.2	4.3	6.0	4.5	4.7	6.5	5.0	5.1	7.1	5.5	5.6	7.9	12.9	13.3	18.5
Gifurwe	110/30	10	0.8	0.8	1.1	0.8	0.9	1.2	0.9	0.9	1.3	1.0	1.0	1.5	2.4	2.5	3.4
Nyabihu	110/30	20	-	-	-	4.0	4.1	5.7	4.4	4.5	6.3	4.8	5.0	6.9	11.4	11.8	16.4
Total			19.3	19.9	27.7	24.8	25.5	35.6	27.3	28.1	39.2	30.0	30.9	43.1	70.8	72.9	101.6
Eastern Zone																	
Kabarondo	110/30	20	5.7	5.9	8.2	6.2	6.3	8.8	6.8	7.0	9.7	7.4	7.7	10.7	21.3	21.9	30.6
Rwinkwavu	110/15	6	2.2	2.3	3.2	2.4	2.5	3.5	2.7	2.7	3.8	2.9	3.0	4.2	6.9	7.1	9.9
Musha	110/15	10	12.3	12.7	17.7	13.3	13.7	19.1	14.6	15.0	21.0	16.1	16.5	23.1	37.9	39.0	54.4
Gabiro	110/30	20	2.8	2.9	4.0	3.0	3.1	4.3	3.3	3.4	4.7	3.6	3.7	5.2	8.5	8.8	12.2
Nyamugari (New)	220/11	30	-	-	-	-	-	-	-	-	-	-	-	-	0.8	0.8	1.1
Total			23.0	23.7	33.1	24.8	25.6	35.6	27.3	28.1	39.2	30.0	30.9	43.1	75.3	77.6	108.1

Note:

- P are in MW
- Q is in MVar
- S is in MVA
- Average load power factor is 0.8.